ISSN 8755-6839

SCIENCE OF **TSUNAMI HAZARDS**

Journal of Tsunami Society International

Volume 38 **Number 3** **2019**

TSUNAMI SOCIETY INTERNATIONAL, 1741 Ala Moana Blvd. #70, Honolulu, HI 96815, USA.

SCIENCE OF TSUNAMI HAZARDS is a CERTIFIED OPEN ACCESS Journal included in the prestigious international academic journal database DOAJ, maintained by the University of Lund in Sweden with the support of the European Union. SCIENCE OF TSUNAMI HAZARDS is also preserved, archived and disseminated by the National Library, The Hague, NETHERLANDS, the Library of Congress, Washington D.C., USA, the Electronic Library of Los Alamos, National Laboratory, New Mexico, USA, the EBSCO Publishing databases and ELSEVIER Publishing in Amsterdam. The vast dissemination gives the journal additional global exposure and readership in 90% of the academic institutions worldwide, including nation-wide access to databases in more than 70 countries.

OBJECTIVE: Tsunami Society International publishes this interdisciplinary journal to increase and disseminate knowledge about tsunamis and their hazards.

DISCLAIMER: Although the articles in SCIENCE OF TSUNAMI HAZARDS have been technically reviewed by peers, Tsunami Society International is not responsible for the veracity of any statement, opinion or consequences.

Submit manuscripts of research papers, notes or letters to the Editor. If a research paper is accepted for publication the author(s) must submit a scan-ready manuscript, a Doc, TeX or a PDF file in the journal format. Issues of the journal are published electronically in PDF format. There is a minimal publication fee for authors who are members of Tsunami Society International for three years and slightly higher for non-members. Tsunami Society International members are notified by e-mail when a new issue is available. Permission to use figures, tables and brief excerpts from this journal in scientific and educational works is granted provided that the source is acknowledged.

Recent and all past journal issues are available at: http://www.TsunamiSociety.org CD-ROMs of past volumes may be purchased by contacting Tsunami Society International at postmaster@tsunamisociety.org Issues of the journal from 1982 thru 2005 are also available in PDF format at the US Los Alamos National Laboratory Library http://epubs.lanl.gov/tsunami/

WWW.TSUNAMISOCIETY.ORG

ISSN 8755-6839

SCIENCE OF TSUNAMI HAZARDS

Journal of Tsunami Society International

Volume 38 Number 3 2019

POTENTIAL TSUNAMI HAZARD RELATED TO THE SEISMIC ACTIVITY EAST OF MAYOTTE ISLAND, COMOROS ARCHIPELAGO

Jean Roger[1,*]

1. LEGOS, Institut de Recherche pour le Développement, 101, Promenade Roger Laroque, BP A5 98848 Nouméa Cedex (contact: jeanrog@hotmail.fr) (Received May 28, 2019, Accepted for publication June 4, 2019)

ABSTRACT

On May 13, 2018, a seismic swarm began to occur east of Mayotte Island, Comoros Archipelago. Only two days after, a strong Mw 5.9 earthquake shook the island and awakened the fears of local people to be struck by a tsunami, in the aftermath of the catastrophic 2004 Indian Ocean event. This paper does not claim to represent a detailed tsunami hazard study, but tries to provide keys about the potential of tsunami generation in the area, explaining point by point the capacity of each source, earthquake, submarine volcanic eruption and landslide to produce perturbation of the sea. Numerical modelling of landslide is presented herein to discuss the relative immunity offered by the coral barrier reef to the island populated coastline to moderate scenarios

1. GENERAL SETTINGS

1a. *Geology*

Mayotte *'Maore'* is a little French island of 374 km² belonging to the Comoros Archipelago, *the islands of the Moon*, at the northern outskirt of the Mozambique Channel, separating Madagascar from Africa (**Fig. 1a**). This archipelago is the surface geological result of a volcanic hotspot beginning to build volcanoes between 15 and 10 million years ago, with an emerged part about 8 to 10 million years ago (**Debeuf, 2009**). Some authors propose a combined tectonic activity on transform faults reactivated by a lithospheric deformation (**Nougier et al., 1986; Michon, 2016**). Mayotte is a volcanic structure rising at least 4400 m above the sea floor (**Audru et al., 2006**), showing a maximum altitude of 660 m a.s.l. only at Mount Bénara (Fig. 1b).

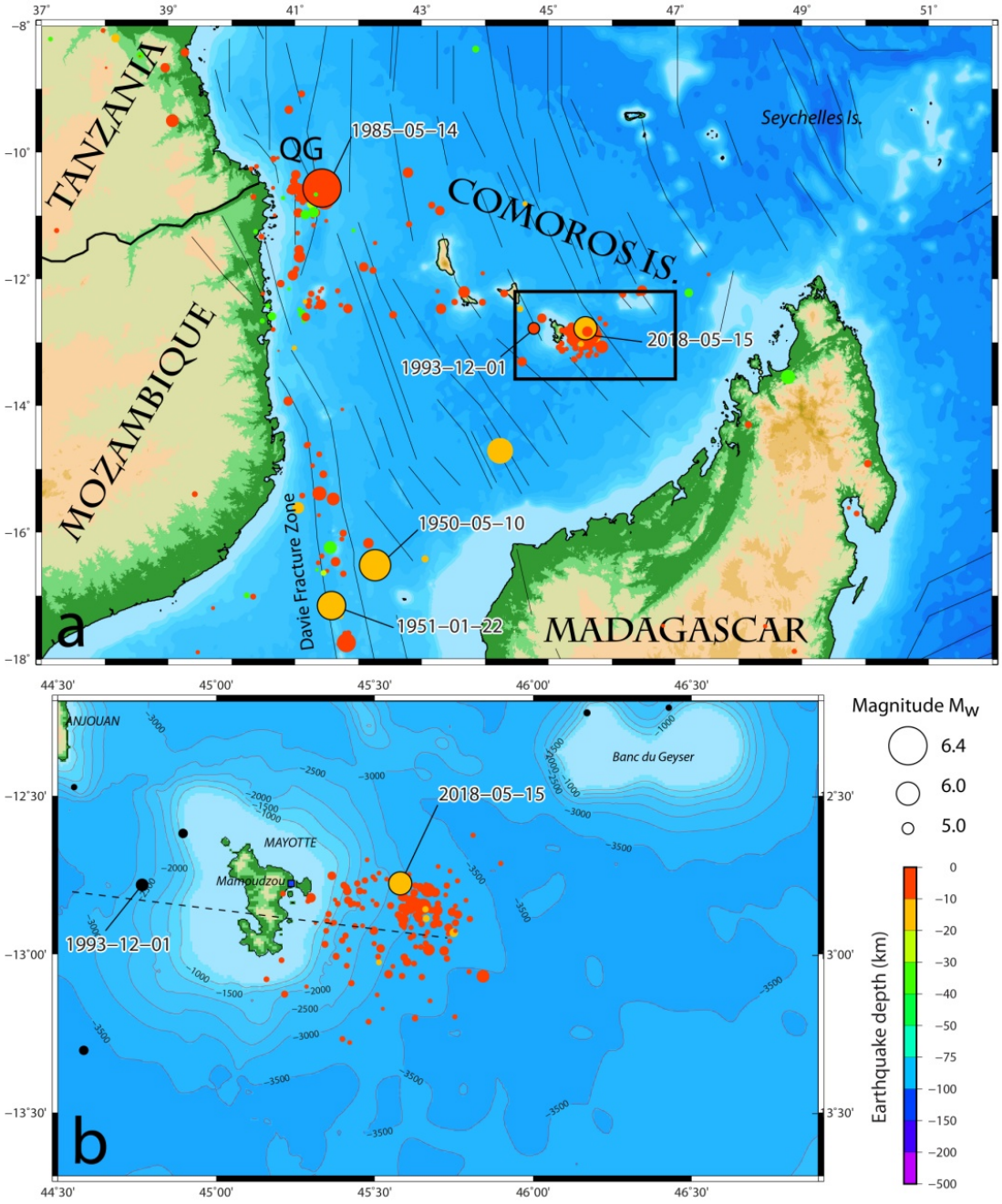

Figure 1: Geologic settings. a) Mayotte is an island of the Comoros Archipelago located within the Mozambique Channel between Madagascar and Mozambique; earthquake epicenters recorded by the USGS since 1950 are shown by colored circles, the size of which is a function of earthquake magnitude; black segments: fractures identified by Phethean et al. (2016). b) Focus on the earthquake swarm since May 15, 2018; black dots: seismic activity before May 15, 2018; black dashed line: profile location shown on figure 2.

The volcanic activity moved progressively toward the North-West, and is now located in Grande Comore. It resulted in the stop of the island growth, which, coupled to an active tropical erosion due to heavy rainfall, led to its subsidence and the slow construction of a coral reef around Mayotte. The lagoon surface is estimated to ~1500 km^2 lagoon, being among the largest in the world.

1b. ***Population and natural hazards***

Mayotte is a highly populated island relative to its available living surface: in 2017, the population density was estimated to 690 people per square kilometer, rising at a rate of 3.8 % per year (**Genay and Merceron, 2017**).

Until May 2018, amongst the natural hazards commonly affecting Mayotte like heavy rains, storms or landslides, was not the ground shaking or earthquake : in fact, **Audru et al. (2010)** indicate that the French SisFrance earthquake catalog reports only 3 events in 1936, 1941 and 1953 to add to the USGS database, which itself shows only two other recorded events: the Mw 5.2 December 1, 1993 and the Mw 5.0 September 9, 2011 earthquakes. Thus, the island population is not historically prepared for earthquakes as it is the case in very active regions like subduction zones.

1c. ***The earthquake swarm***

On May 13, 2018, a magnitude Mw 4.6 earthquake was widely felt by the island population. It was the first noticeable event of the ongoing earthquake swarm beginning on May 10, 2018 according to instrumental records. It was soon followed, two days later on May 15, 2018, by a stronger Mw 5.9 earthquake. This earthquake did not cause any severe damages and did not cause any severe injuries (only 3 wounded people were reported by local authorities) but caused the whole population to feel concerned by this natural phenomenon. A range of hypotheses have been raised, and amongst them, the possibility of this swarm to be triggered by submarine volcanic activity. This hypothesis is about to be validated by the recent MAYOBS bathymetric survey from a French consortium of research laboratories. The problem in this area is that the geology and tectonics are not very well constrained, and the lack of geophysical data (and especially seismic data) from local stations generates uncertainties concerning the swarm interpretation.

As a result, the population is afraid of what could happen in the near future and lots of people wonder if such an earthquake could be able to trigger a tsunami toward the island coasts, remembering the 2004 Indian Ocean catastrophic event.

1d. ***Historical tsunamis***

Mayotte is not an island known to have been affected severely by tsunamis over the past centuries, but this could simply be a consequence of insufficient written archives. Thus, two events have been reported there recently the November 27, 1945 Makran (Iran) tsunami and the December 26, 2004 Sumatra ocean-wide tsunami (**Lambert and Terrier, 2011**). The first one shows a run-up of 4.05 m in Mayotte and more than 6 m in the neighboring island of Grande Comore (**Okal et al., 2009**). The second one affected the northwestern part of the Indian Ocean, as for example the Seychelles Islands where it has been reported to 30-50 cm (**Heidarzadeh and Satake, 2014**). For information, it also reached about 1 m at Mtsanga Safari

beach on Chissoua Mtsamboro, north of Mayotte (**Matthias Deuss, pers. comm., 2019**) although **Lavigne et al. (2012)** indicate there is no real evidence on Mayotte coastline. Nevertheless, the 2004 event, and all the catastrophic tsunamis that occurred thereafter, have severely impressed the world's population, especially those who are living in coastal areas. Such is the case in Mayotte, where the coastal population is rising wildly (**Bernardie-Tahir and El-Mahaboubi, 2001**): people are now very concerned by natural hazards, amid fears of the ability of the earthquakes to trigger destructive tsunami waves.

2. DIFFERENT ORIGINS

2a. *"Earthquake tsunami"*

On March 21, 2019, the earthquake swarm was composed of 16 earthquakes of magnitude Mw ≥ 5 and 161 with 4.0 ≤ Mw < 5.0 according to the USGS database (**U.S. Geological Survey, 2019**).Global tsunami databases such as the NOAA NGDC/WDS tsunami catalogue (www.ngdc.noaa.gov/hazard/tsu_db.shtml) or the Historical Tsunami Database for the World Ocean -HTDB/WLD (http://tsun.sscc.ru/tsunami-database/index.php) allow to empirically show that there are no recorded tsunamis triggered by earthquakes of magnitude Mw < 6.3 (**Tinti, 1991**). Given that the biggest earthquake of the Mayotte swarm reached only a moment magnitude Mw = 5.9, it was normally not sufficient to trigger a tsunami. **Bolt et al. (1975)**, for example, have indicated that the maximum run-up for a tsunami generated by a Mw = 6.5 earthquake would be no more than 0.5-0.75 m.

In addition, the moment tensors calculated by the Global CMT project (https://globalcmt.org) for the major earthquakes of the seismic swarm exhibit strike-slip mechanisms showing sometimes very limited normal or reverse components. Most of the strike-slip events recorded around the World have not been able to trigger tsunamis but **Tanioka and Satake (1996)** have shown that, in cases where the rupture occurs on a steep slope with a horizontal displacement significantly larger than the vertical displacement, horizontal movement -strike-slip faulting- along a fault plane is also able to trigger a tsunami. In addition, **Legg and Borrero (2001)** and **Borrero et al. (2004)** have also shown that tectonic events occurring on strike-slip faults with sinuous traces could trigger tsunamis by the effect of uplift and subsidence along successions of fault bends and releasing bends. In the case of a substantial increase of earthquakes magnitude (Mw > 6.3-6.5) in the swarm area, it would be difficult for a strike-slip mechanism to produce such displacement as most of the earthquake epicenters have been located under the abyssal plain, i.e. in an area where no submarine features like grabens or seamounts have been identified (this information could change after the mapping of the discovered volcanic structure by the MAYOBS survey). In addition, the structures identified by Phethean et al. (2016) and shown on figure 1a seem not able to produce magnitudes sufficient to trigger tsunamis but should be clarified with seismic data.

2b. *"Volcanic tsunami"*

Volcanic eruptions are also able to trigger tsunamis: 123 of the 2640 tsunamis reported in the NOAA NGDC/WDS tsunami catalogue are attributed to volcanic eruptions, i.e. 4.65 % of the reported tsunamis. About 29% are the results of submarine explosions (**Latter, 1981**) but a handful of them are amongst them, the biggest catastrophic tsunamis like the emblematic eruption of the Krakatoa, Indonesia, on August 26,

1883, which was able to trigger a 15 m high wave on both side of the Sunda Strait, reaching 40 m in some places and killing thousands (**Nomanbhoy and Satake, 1995; Pelinovsky et al., 2005**). In addition, the structures identified by Phethean et. al. (2016) and shown on figure 1a seem not able to produce magnitudes sufficient to trigger tsunamis and should be clarified with seismic data.

Another catastrophic event is the Santorini, Greece, explosion circa 1470 BC and having triggered a powerful tsunami with impacts on nearby islands. But most of the time, the tsunamis following volcanic eruptions are triggered not by the explosion itself as in the two previous cases, but because of induced landslides, rock falls or pyroclastic flows. In order to understand the tsunami generation mechanism by underwater explosions only a few studies like the ones by **Duffy (1992)** and **Egorov (2007)** have been conducted over the past decades, probably because tide gauge data for such tsunamis are seriously lacking (**Belousov et al., 2000**). Nevertheless, in case an underwater explosion occurs it has been shown that the generation of a tsunami is directly linked to thresholds of heterogeneous and homogeneous hydroexplosion related to water depths of respectively 675 m and 130 m (**Smith and Shepherd, 1993**). Considering this study, in the specific case of Mayotte, if the submarine volcanic structure identified by the MAYOBS survey in the swarm area turns out to be linked to the earthquakes, it corresponds to a ~800 m high edifice lying on depths of ~2500-3000 m, and thus, it is unlikely for such a scenario to occur. But as detailed by **Paris (2015),** all submarine eruptions show different behavior and the depth of the volcano is not the only parameter to consider in the equation. For example, the author indicates that the caldera collapse duration could also be an important factor to deal with.

2c. *"Landslide tsunami"*

Landslides are relatively frequent events occurring at active continental margins or on the slopes of oceanic islands, especially if these islands are located into areas of plate convergence. Tsunamis generated by landslides are quite common and these landslides could be associated with other natural hazards like heavy rainfall, earthquakes or volcanic eruptions. Tsunamis triggered by landslides show the most impressive amplitudes and run-up heights, especially events like the 1958 tsunami in Lituya Bay, Alaska, which attained a maximum run-up limit of 524 m above mean sea level (**Gonzalez-Vida et al., 2019**). But although they could show high amplitudes near the source, they are also prone to important energy dispersion phenomenon. It is important to note that a large number of massive landslide-triggered tsunamis have been caused by earthquakes like the 1929 Grand Bank, Newfoundland or the more recent December 2018 Anak Krakatau, Indonesia events.

In the present case study, it is worth noting that landslides would occur mainly on the slopes of Mayotte Island itself. The BATHYMAY survey (**Audru et al., 2006**) has highlighted the presence of steep slope angles in excess of 15° (as shown on **figure 2**) and numerous submarine canyons, in addition to well identified faults network, sometimes striking through the barrier reef. It is thus easy to imagine that the multitude of earthquakes of the swarm probably affected the stability of these slopes, especially the earthquakes located closest to the island (westernmost events) and showing the strongest intensities.

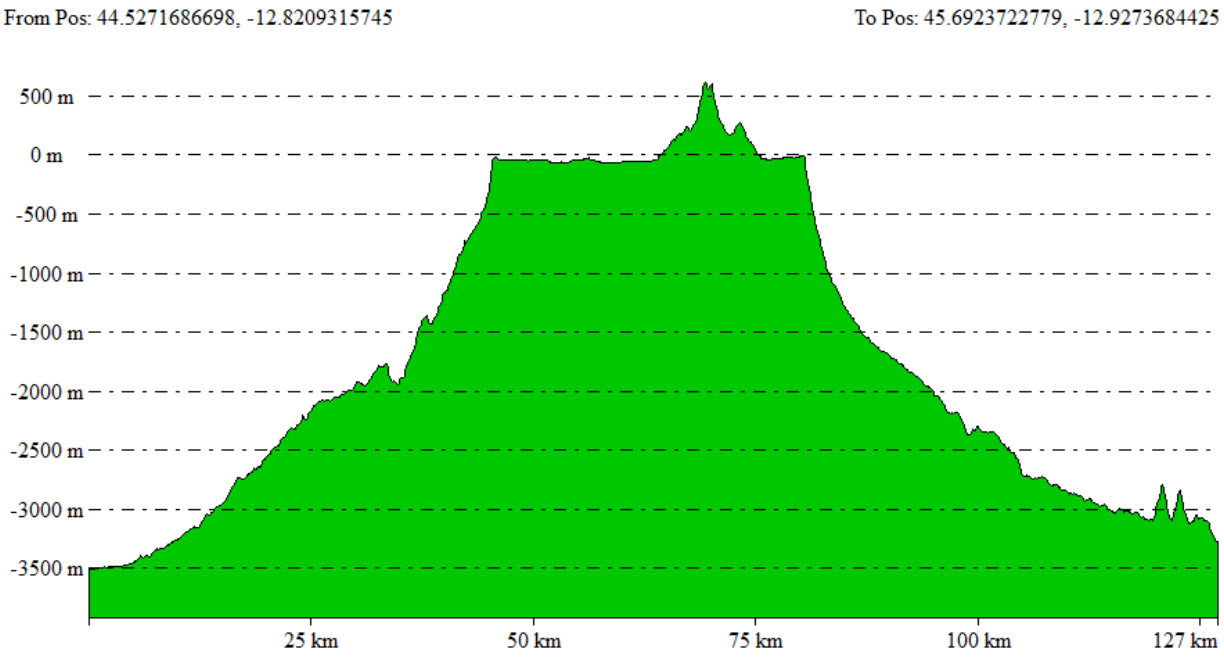

Figure 2: Cross profile of Mayotte D.E.M. (associated to SRTM topographic data) showing steep slopes. The profile location is indicated in figure 1. Bathymetric data are from the SHOM (2016) and Topographic data above sea level are SRTM 3 arcseconds data.

In case a landslide occurred very close to the island, it would be important to determine in what proportion the barrier reef (if not part of the landslide) and lagoon width would play a protective role, attenuating the wave energy by way of energy dispersion and friction occurring at the lagoon floor.

3. NUMERICAL MODELING

Tsunami modeling is used to estimate the role played by the coral reef and the lagoon surrounding Mayotte Island during the tsunami propagation. The objective is not to propose a set of scenarios to produce hazard maps but to discuss the capacity of a tsunami triggered by a submarine landslide to impact Mayotte coastline. For this purpose, only two different cases of relevant submarine landslide scenarios are detailed.

3a. *GEOWAVE*

The modelings was carried out using GEOWAVE software. This is a package consisting of two different modules: the TOPICS module, which computes the initial deformation of the sea floor with different options of slope mass movements (debris flow, rotational slump, etc.); and the FUNWAVE module, in which this initial deformation is introduced as an input for computing the tsunami propagation and inundation if needed (**Watts et al., 2003**). The robustness and accuracy of GEOWAVE have been validated through numerous studies all around the world (e.g. **Watts et al., 2003; Ioualalen et al., 2006; Grilli et al., 2007; Watts and Tappin, 2012**). In the specific case of landslide modeling, it is interesting to indicate that the model uses a finite element scheme to solve the non-linear Boussinesq equations and considers dispersion behavior.

3b. *Digital Elevation Model*

As an input to the model, a digital elevation model (D.E.M.) showing a resolution of ~180 m was prepared by degrading the available 0.001° resolution D.E.M. from the SHOM (French Navy Oceanographic and Hydrographic Office; **SHOM, 2016**), and was combined with SRTM 3 arcseconds data (~90m at the equator; **Jarvis et al., 2008**) for land topography. This resolution was chosen to answer both to the software calculation limitations and to reproduce the underwater features and the coral barrier surrounding the island as well as possible. The resulting D.E.M. is presented on figure 3.

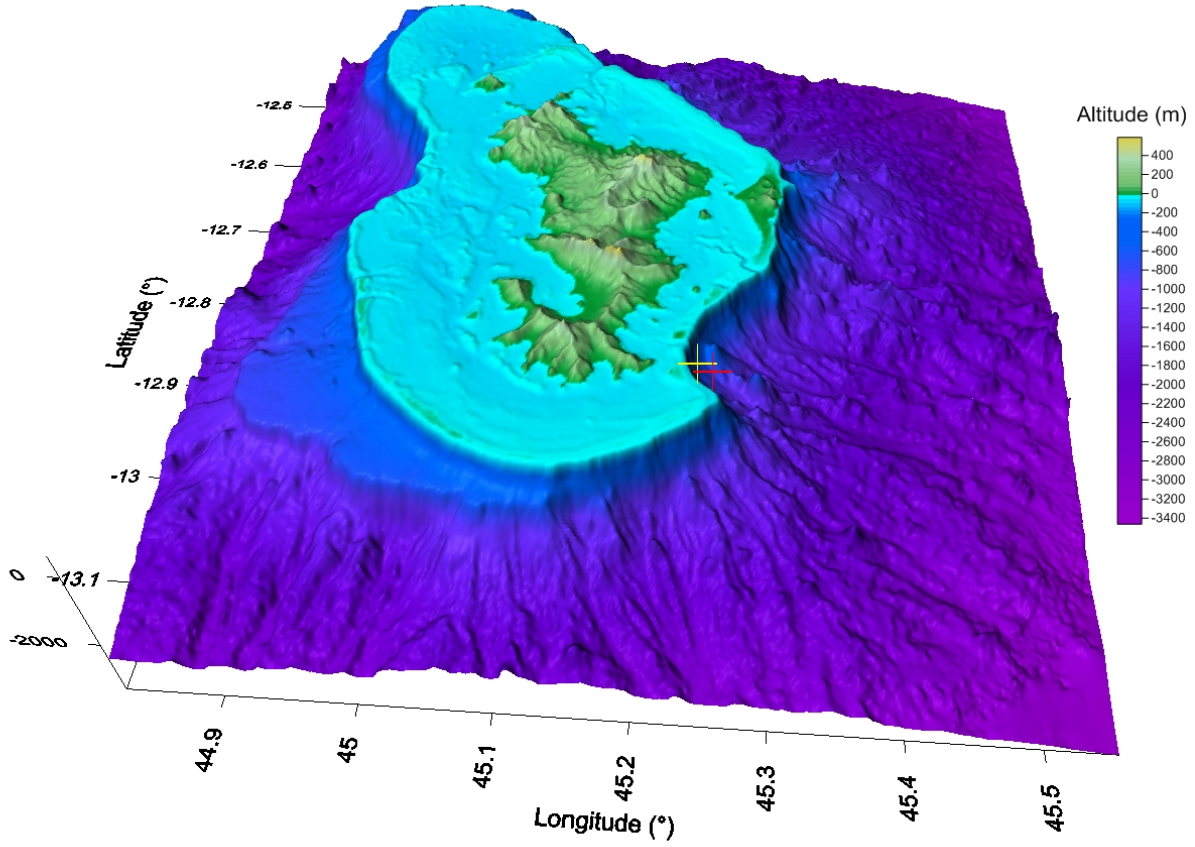

Figure 3 : 180 m resolution digital elevation model (D.E.M.) of Mayotte Island prepared with bathymetric data from the SHOM and SRTM topographic data. Yellow and red crosses locate respectively V1 and V2 landslide gravity centroids used in the modeling.

3c. *Scenarios*

It is important to consider the local geology before modeling underwater landslides. The numerical modeling software needs some source parameters to compute the initial deformation surface. In this case, it has been decided to consider rotational slump behavior in agreement with available literature about landslides on volcanic islands (e.g. **Whelan and Kelletat, 2003**).

The most important parameter of a landslide for triggering a tsunami is its initial velocity (**Lovholt et al., 2015**), which itself is directly linked to the volume and density of the moving material and to slope angle. The volume depends on the characteristic length L, width W and thickness T of the sliding material. The ratios between these parameters are consistent with previous studies (e.g. **Yamagishi and Ito, 1994**).

According to the fact that Mayotte is a volcanic island surrounded by a well-developed calcareous reef, the bulk density of the sliding of potentially unconsolidated material has been arbitrarily chosen as 2000 kg/m^3, a plausibly low value of water-saturated sandstone bulk density (**Manger, 1963**). Run-out distances have been chosen to stay within the stability window of GEOWAVE.

We chose to model two landslide scenarios located on the south-east flank of the island (yellow and red crosses in **Figure 3**) in a region where the shape of the bathymetry could be associated to one or several submarine landslides. The parameters of the two landslides are given in **Table 1**.

The volumes have been chosen in agreement with available literature about submarine landslides and correspond to "classical" medium-size slope-failure events of respectively 0.012 and 0.12 km^3.

Scenario	V1	V2
V (km3)	0.012	0.12
x_0 (°)	45.24°E	45.25°E
y_0 (°)	-12.97	-12.97
d (m)	560	800
L (m)	600	1500
W (m)	400	400
T (m)	50	200
Φ (°)	270	270
Θ (°)	16	16
MWH(m)	0.69	3.21

Table 1: Parameters for the two rotational slump scenarii as introduced in GEOWAVE. V corresponds to the landslide volume, x0, y0 and d to the longitude, latitude and depth of the center of mass, L, W and T to the length, width and thickness of the volume, Φ to the azimuth and Θ to the slope angle. MWH represents the maximum value of the sea level reached at one node of the grid.

4. RESULTS

The two scenarios have been modeled with GEOWAVE for a propagation time of 30 minutes over the 180 m resolution D.E.M.

Figure 4 shows numerical propagation of the tsunami triggered by scenario V2. It highlights the propagation of a ~3 m high tsunami (maximum value = 3.21 m) in an isotropic way (except for the lagoon part, in the west) from the first seconds to 28 minutes of the model run. At the very first time of the propagation (= first minute), the shape of the tsunami is directly related to the landslide parameters including the runout length. In the present case it shows a "flying bird" shape produced by the moving material toward the east that will evolve quickly to an alternating pattern of peaks and troughs radiating from the source region.

It shows clearly that after less than 30 minutes, and due to wave dispersion and wrapping around the barrier reef, the energy loss leads to tsunami disappearance (amplitude goes from 3 m to less than 5 cm).

The wave train entering the lagoon reaches the coastline in less than 10 minutes, travel time directly linked to the lagoon width and depth in front of the source location.

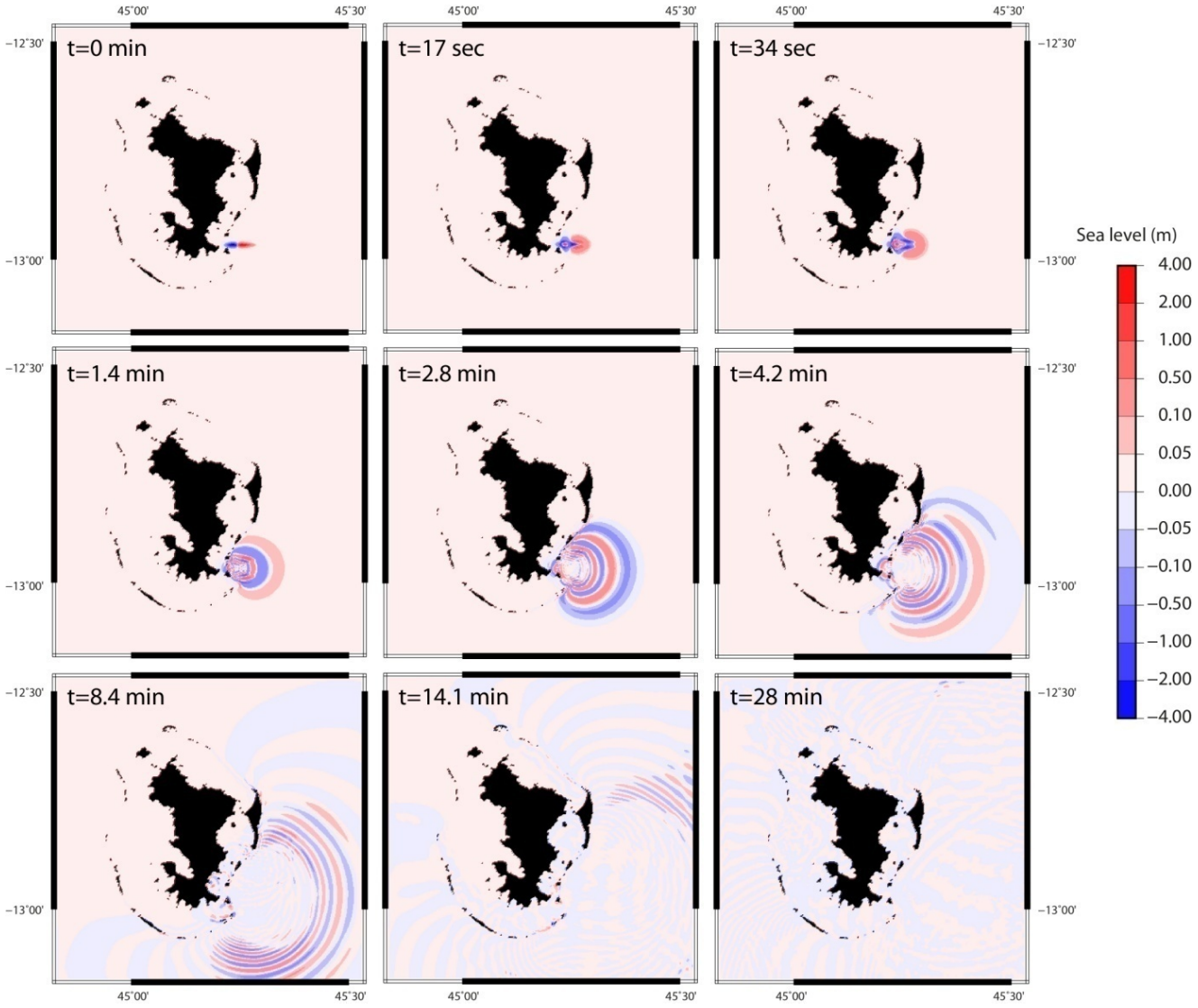

Figure 4 : Propagation of a tsunami triggered by a landslide on Mayotte Island southeastern slope.

Figure 5 presents the maximum wave heights maps for scenarii V1 and V2 representing the maximum wave height reached on each nodes of the grid during the whole propagation. As during the propagation process, the "flying bird" shape is also associated to the maximum wave heights recorded on the whole grid with value ranging between 0.4 and 1 m for scenario V1 and between 1 and 3.2 m for scenario V2. In both cases, the high values shown on the west of the source, close to the barrier reef, correspond to wave shoaling when the water depth decreases on the island slope.

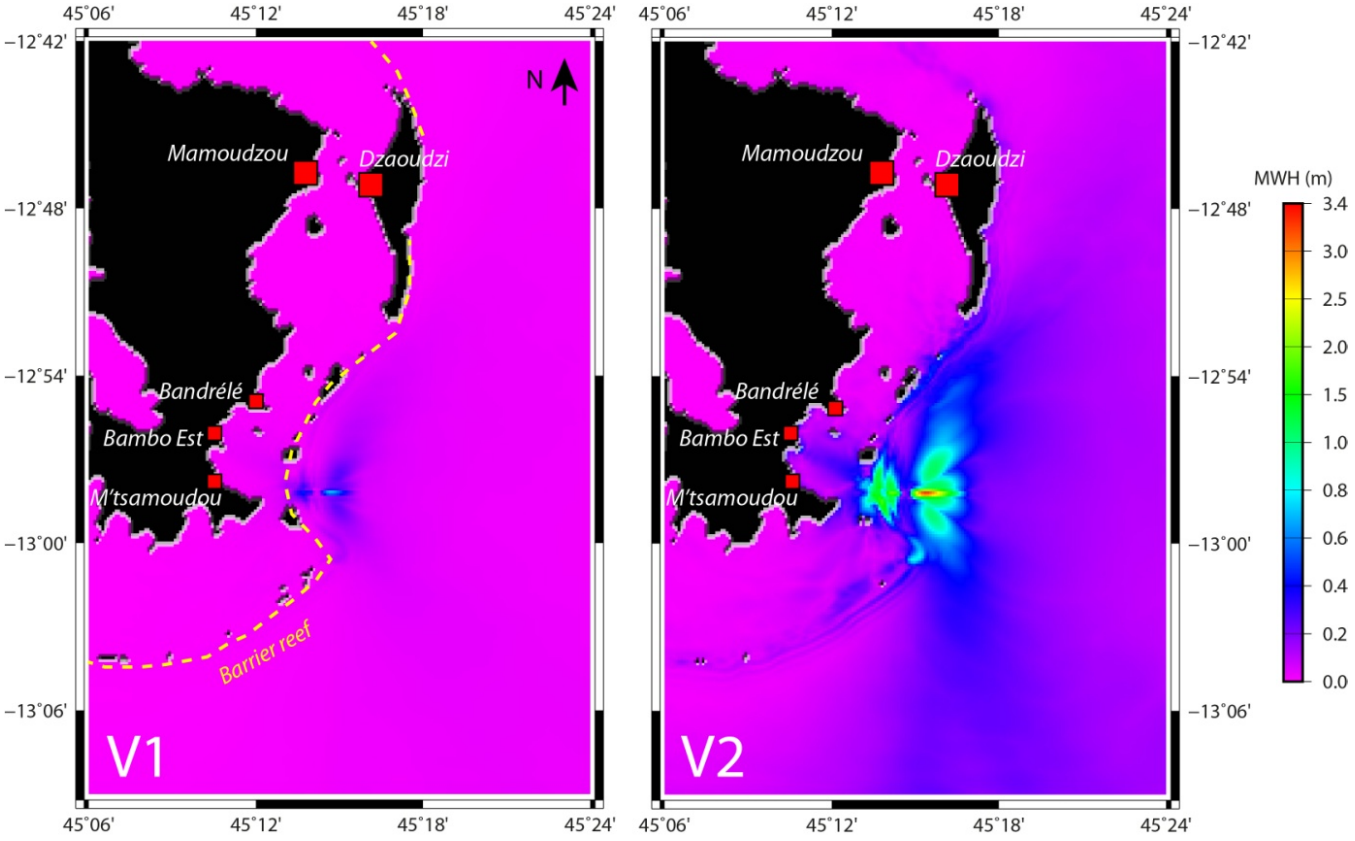

Figure 5: Focus on the maximum wave height maps (MWH) for V1 and V2 scenarii in the source area after 33 min of tsunami propagation. Some towns and villages are symbolized with red squares. Yellow dashed line: coral barrier reef.

Except the difference of wave heights and dispersion between the two scenarios, it reveals that in such cases:

- the barrier reef plays a protective role against tsunami waves triggered by landslides (showing high frequency waves in comparison to tsunamis triggered by earthquakes): in the case of scenario V1, there is no significant sea level change inside the lagoon and for scenario V2, the maximum height is divided by at least 6 from 3.2 m (maximum value) to 0.5 m maximum inside the lagoon;

- the maximum wave heights do not exceed 0.5 m at a distance of circa 10 km away from the source (scenario V2).

5. CONCLUSIONS

This study indicates that the actual knowledge of the geology in Mayotte region, including the recent discovery of a submarine volcano within the seismic swarm area east of the island, enable to conclude that neither an earthquake within the actual magnitude range (Mw < 6.0), nor a volcanic eruption (at the actual volcano summit depth) could trigger a tsunami having an impact onto the island's coast. However, the numerous earthquakes which seem to be related to the volcanic activity could produce submarine landslides along Mayotte slopes, which landslides are potentially able to trigger tsunamis.

Currently, it is not known whether the seismic swarm has been already able to trigger such landslides, even small, along Mayotte. Only small landslides have been identified on land, but those could also be related to frequent heavy rainfalls.

In order to give keys to assess landslide generated tsunami hazard, two landslide scenarii have been modeled. The results of tsunami modeling presented hereabove show that the tsunami shape and coastal impact are directly linked to the volume of the landslide as already demonstrated by numerous studies in other regions. They also highlight the role played by the coral barrier reef in terms of mitigation of the tsunami hazard, and this information should be considered by decision-makers to protect these valuable ecosystem surrounding Mayotte.

It is important to notice that the two modeled scenarii are based on available literature on submarine landslides and not on geological facts reported around Mayotte. The objective was only to estimate what could happen in case an earthquake destabilizes unconsolidated sediments or a part of the barrier reef. To make an accurate hazard study about tsunamis triggered by landslides, the first most important thing would be to identify all scars of past landslides that could exist along the island margin and estimate the mobilized volumes. The second step would be to identify and map the potential unstable areas, if they exist, and to propose realistic volumes for each one. These values could then be entered as data in further model runs. In addition, the tide level should also be considered as Mayotte is subject to a maximum tidal range of ~4 m, modeling the same tsunamis at low and high tides.

ACKNOWLEDGMENTS

The author is very grateful to Yanni Gunnell who kindly proofread the manuscript.

Funding

This study has not been funded.

REFERENCES

Audru, J.-C., Bitri, A., Desprats, J.-F., Dominique, P., Eucher, G., Hachim, S., Jossot, O., Mathon, C., Nédellec, J.-L., Sabourault, P., Sedan, O., Stollsteiner, P., Terroer-Sedan, M. (2010). Major natural hazards in a tropical volcanic island: A review for Mayotte Island, Comoros archipelago, Indian Ocean. Engineering Geology, 114, 364-381.

Audru, J.-C., Guennoc, P., Thinon, I., Abellard, O. (2006). BATHYMAY: underwater structure of Mayotte Island revealed by multibeam bathymetry. Comptes-Rendus Geosciences, 338(16), 1240-1249.

Belousov, A., Voight, B., Belousova, M., Muravyev, Y. (2000). Tsunamis generated by subaquatic volcanic explosions: unique data from 1996 eruption in Karymskoye Lake, Kamchatka, Russia. Pure and Applied Geophysics, 157, 1135-1143.

Bernardie-Tahir, N., El-Mahaboubi, O. (2001). Mayotte: des parfums au tourisme. Les nouveaux enjeux du littoral. Les Cahiers d'Outre-Mer, 216, 369-396.

Bolt, B.A., Horn, W.L., Macdonald, G.A., Scott, R.F. (1975). Geological Hazards. Earthquakes - Tsunamis - Volcanoes - Avalanches - Landslides - Floods. Springer-Verlag, 329 pp., 116 fig., doi : 10.1007/978-3-642-86820-7.

Borrero, J.C., Legg, M.R., Synolakis, C.E. (2004). Tsunami sources in the southern California bight. GeophysicalResearchLetters, 31(13), L13211, doi : 10.1029/2004GL020078.

Debeuf, D. (2009). Etude de l'évolution volcano-structurale et magmatique de Mayotte, archipel des Comores, océan Indien: approche structurale, pétrographique, géochimique et géochronologique. Thèse de volcanologie, Université de la Réunion, 277 pp.

Duffy, D.G. (1992). On the generation of oceanic surface waves by underwater volcanic explosions. Journal of Volcanology and Geothermal Research, 50(3), 323-344, https://doi.org/10.1016/0377-0273(92)90100-R.

Egorov, Y. (2007). Tsunami wave generation by the eruption of underwater volcano. Natural Hazards and Earth System Sciences, 7, 65-69.

Genay, V., Merceron, S. (2017). 256500 habitants à Mayotte en 2017. INSEE FOCUS, 105, https://www.insee.fr/fr/statistiques/3286558.

Gonzalez-Vida, J., Macias, J., Castro, M.J., Sanchez-Linares, C., de la Asuncion, M., Ortega-Acosta, S., Arcas, D. (2019). The Lituya Bay landslide-generated mega-tsunami - numerical simulation and sensitivity analysis. Natural Hazards and Earth System Sciences, 19, 369-388.

Grilli, S.T., Ioualalen, M., Asavanant, J., Shi, F., Kirby, J.T., Watts, P. (2007). Source constraints and model simulation of the December 26, 2004 Indian Ocean tsunami. Journal of Waterways, Port, Coastal and Ocean Engineering, 133(6), https://doi.org/10.1061/(ASCE)0733-950X(2007)133:6(414).

Heidarzadeh, M., Satake, K. (2014). New insights into the source of the Makran tsunami of 27 November 1945 from tsunami waveforms and coastal deformation data. Pure and Applied Geophysics, 172(3-4), 621-640, https://doi.org/10.1007/s00024-014-0948-y.

Ioualalen, M., Pelletier, B., Watts, P., Regnier, M. (2006). Numerical modeling of the 26th November 1999 Vanuatu tsunami. Journal of Geophysical Research, 111, C06030, https://doi.org/10.1029/2005JC003249.

Ioualalen, M., Asavanant, J., Kaewbanjak, N., Grilli, S.T., Kirby, J.T., Watts, P. (2007). Modeling the 26 December 2004 Indian Ocean tsunami: Case study of impact in Thailand. Journal of Geophysical Research, 112, C07024, https://doi.org/10.1029/2006JC003850.

Jarvis, A., Reuter, H.I., Nelson, A., Guevara, E. (2008). Hole-filled SRTM for the globe Version 4, available from the CGIAR-CSI SRTM 90M Database (http://srtm.csi.cgiar.org).

Lambert, J., Terrier, M. (2011). Historical tsunami database for France and its overseas territories. natural Hazards and Earth System Sciences, 11, 1037-1046.

Latter, J.H. (1981). Tsunamis of volcanic origin: Summary of causes, with particular reference to Krakatoa, 1883. Bulletin of Volcanology, 44(3), 467-490.

Lavigne, F., Sahal, A., Coquet, M., Wassmer, P., Goett, H., Leone, F., Péroche, M., Lagahé, E., Gherardi, M., Vinet, F., Hachim, S., Drouet, F., Quentel, E., Loevenbruck, A., Schindelé, F., Hébert, H., Anselme, B., Durand, P., Gaultier-Gaillard, S., Pratlong, F., Divialle, F., Morin, J. (2012). PREPARTOI. Final Report, 257 pp.

Legg, M.R., Borrero, J.C. (2001). Tsunami potential of major restraining bends along submarine strike-slip faults. ITS 2001 Proceedings, session 1, Number 1-9, 331-342.

LØvholt, F., Pedersen, G., Harbitz, C.B., Glimsdal, S., Kim, J. (2015). On the characteristics of landslide tsunamis. Philosophical Transactions A, Math. Phys. Eng. Sci., 373(2053), 20140376, https://doi.org/10.1098/rsta.2014.0376.

Nomanbhoy, N., Satake, K. (1995). Generation mechnism of tsunamis from the 1883 Krakatau eruption. Geophysical Research Letters, 22(4), 509-512.

Nougier, J., Cantagrel, J.M., Karche, J.P. (1986). The Comores archipelago in the western Indian Ocean: volcanology, geochronology and geodynamic setting. Journal of African Earth Sciences, 5(2), 135-145.

Manger, G.E. (1963). Porosity and bulk density of sedimentary rocks. Contributions to geochemistry. Geological Survey Bulletin, 1144-E

Michon, L. (2016). The volcanism of the Comoros archipelago integrated at a regional scale. In: Bachelery, P., Lénat, J.-F., Di Muro, A. and Michon, L. (Eds.), Active Volcanoes of the Southwest Indian Ocean: Piton de la Fournaise and Karthala, Springer-Verlag, 233-244, Active Volcanoes in the World, 978-3-642-31394-3.

Okal, E.A., Fritz, H.M., Sladen, A. (2009). 2004 Sumatra-Andaman tsunami surveys in the Comoro Islands and Tanzania and regional tsunami hazard from future Sumatra events. South African Journal of Geology, 112, 343-358.

Paris, R. (2015). Source mechanisms of volcanic tsunamis. Philosophical Transactions of the Royal Society A, 373, 20140380, http://dx.doi.org/10.1098/rsta.2014.0380.

Pelinovsky, E., Choi, B.H., Stromkov, A., Didenkulova, I., Kim, H.-S. (2005). Analysis of tide-gauge records of the 1883 Krakatau tsunami. In: Satake, K. (eds): Tsunamis. Advances in Natural and Technological Hazards Research, Springer, 23, 57-77.

Phethean, J.J.J., Kalnins, L.M., van Hunen, J., Biffi, P.G., Davies, R.J., McCaffrey, K.J.W. (2016). Madagascar's escape from Africa: A high-resolution plate reconstruction for the Western Somali Basin and implications for supercontinental dispersal. Geochemistry, Geophysics, Geosystems, 17(12), 5036-5055, https://doi.org/10.1002/2016GC006624.

SHOM (2016). MNT bathymétrique de la façade de Mayotte (Projet Homonim). http://dx.doi.org/10.17183/MNT_MAY100m_HOMONIM8WGS84.

Smith, M.S., Shepherd, J.B. (1993). Preliminary investigations of the tsunami hazard of Kick'em Jenny submarine volcano. Natural Hazards, 7, 257-277.

Tanioka, Y., Satake, K. (1996). Tsunami generation by horizontal displacement of ocean bottom. Geophysical Research Letters, 23(8), 861-864.

Tinti, S. (1991). Evaluation of tsunami hazard in Calabria and Eastern Sicily, Italy. In: Tsunamis in the World (Ed.: S. Tinti), 141-157.

U.S. Geological Survey (2019). Earthquake catalogue: accessed March 21, 2019 at URL https://earthquake.usgs.gov/earthquakes/search/.

Watts, P., Grilli, S.T., Kirby, J.T., Fryer, G.J., Tappin, D.R. (2003). Landslide tsunami case studies using a Boussinesq model and a fully nonlinear tsunami generation model. Natural Hazards and Earth System Sciences, 3(5), 391-402.

Watts, P., Tappin, D.R. (2012). Geowave validation with case studies: Accurate geology reproduces observations. In: Yamada Y. et al. (eds) Submarine Mass Movements and Their Consequences. Advances in Natural and Technological Hazards Research, 31, 517-524, https://doi.org/10.1007/978-94-007-2162-3_46.

Whelan, F., Kelletat, D. (2003). Submarine slides on volcanic islands - a source for mega-tsunamis in the quaternary. Progress in Physical Geography, 27(2), 198-216.

Yamagishi, H., Ito, Y. (1994). Relationship of the landslide distribution to geology in Hokkaido, Japan. Engineering Geology, 38(3-4), 189-203, https://doi.org/10.1016/0013-7952(94)90037-X.

ISSN 8755-6839

SCIENCE OF **TSUNAMI HAZARDS**

Journal of Tsunami Society International

Volume 38 **Number 3** **2019**

DEVELOPMENT OF TSUNAMI EARLY WARNING APPLICATION FOUR MINUTES AFTER AN EARTHQUAKE

Madlazim[1], Supriyanto Rohadi[2], Sorja Koesuma[3], Ella Meilianda[4]

e-mail:madlazim@unesa.ac.id

[1]Surabaya State University, Surabaya, INDONESIA

[2]Meteorology Climatology and Geophysics Council, Jakarta, INDONESIA

[3] sebelas Maret University, Solo, INDONESIA

[4] Syiah Kuala University, Aceh, INDONESIA

ABSTRACT

Effective early warning at local to regional distances is maximum 10 minutes after the OT. The shorter the tsunami early warning time that is announced, of course, the more time the community will have to prepare for mitigating the disaster. The purpose of this study is to develop a tsunami application and show the current real-time data available in most tsunami hazard areas in Indonesia - in particular, earthquake location, magnitude and tsunami discriminant Td, T50Ex, T0, Td x T50, and Td x T0 can be determined about four minutes after the earthquake occurs. This process will be implemented and continues in real-time in earthquake monitoring and tsunami early warning installed by the Meteorology Climatology and Geophysics Council. The availability of this rapid tsunami application (about 4 minutes after the OT) can help in tsunami early warning that is faster and more reliable for short distances to areas that have the potential of having the a tsunami impact. The purpose of this study is to produce a tsunami early warning application 4 minutes after the earthquake. The research method used in this study is the ADDIE development method (Analysis, Design, Development, Implementation and Evaluation). In the first year, the focus of the development of rapid tsunami early warning applications was about 4 minutes after the OT. Our previous research results have supported a lot of development this application and make it easier for us to complete the prototype target, it has been obtained the results of the tsunami application prototype 4 minutes after the OT which is currently being tested in real time at the Meteorology Climatology and Geophysics Council Research and Development Center in Jakarta, Indonesia.

Keywords: *tsunami parameters; tsunami early warning; tsunami early warning application; 4 minutes after the earthquake*

Vol. 38, No. 3, page 132 (2019)

1. **INTRODUCTON**

The most destructive tsunamis at close range tsunami-affected areas (eg <1000km) from the epicenter of the earthquake, arrive within 20-30 minutes after the earthquake (OT); Effective early warning at this distance requires notification in less than 10 minutes after OT (eg, Tsushima et al., 2011; Newman et al., 2011; Madlazim, 2011). At present, a rapid assessment of the tsunami potential from earthquake by organizations such as the Meteorology, Climatology and Geophysics Agency (BMKG), Japan Meteorological Agency (JMA), German-Indonesian tsunami warning system (GITEWS) or West Coast and Alaska (WCATWC) and the Pacific (PTWC) depend mainly on the initial estimate of the earthquake location, depth and moment, M0, or the corresponding moment magnitude, Mw. However, reliable Mw calculations for large earthquakes are usually provided by CMT by the tensor-moment tensor power, Mw (Ekström et al., 2005), which requires inversion of waveforms, varying with rupture depth, earth model and other factors, and only available 20-30 minutes or more after an earthquake occurs (Hayes et al., 2011; Duputel et al., 2011). Therefore, fast magnitude estimators such as MWp are used for tsunami CMT warnings, but the Mwp performs poorly compared to Mw and other discriminants for tsunami potential (Lomax and Michelini, 2011A, LM2011; Madlazim, 2011).

To produce effective and efficient tsunami early warning, especially for short distances to potentially tsunami affected areas, we use the tsunami parameter calculation method quickly. We have presented (Lomax and Michelini, 2009B; LM2011; Lomax and Michelini, 2011B; Madlazim, 2011; Madlazim 2013) direct procedures for rapid assessment of potential tsunami earthquake by using direct methods, it is not the inversion of treatment steps on P-wave seismograms - Td dominant period, more than 50 minutes duration, T50Ex, rupture duration, T0. T0 for large earthquakes is mainly related to the length of the rupture, L, and both Td and T0 will increase, the depth of rupture, z, decreases, because the effects of shear modulus and rupture speed, vr are reduced. We have shown (Madlazim 2011; Madlazim 2013) that product multiplication duration Td x T0 or Td x T50Ex provides more information about the impact of tsunami than the Mw, Mwp, Mwpd discriminant (Lomax and Michelini, 2009A, LM2009A; Madlazim. 2011; Madlazim 2013), and other currently used discriminants. These results indicate that the tsunami potential is not directly related to the product L x W x D of the "seismic" fault model, as assumed by the use of Mw discriminant so far and suggest that information about length and depth can explain the tsunami potential of an earthquake well. Information about the rupture's length and depth is provided by TD x T0 and Td x T50Ex, where explicit estimation of the rupture's length and depth are difficult and cannot be determined quickly.

Until today, the earthquake and tsunami early warnings continue to be developed to get a more accurate and faster earthquake and tsunami early warning system. Effective tsunami early warning for coastlines at regional distances (> 500 km) from the epicenter of the earthquake that creates a tsunami requires notification within 15 minutes after the earthquake. Recently, through analysis of P-wave tele-seismic seismograms (30º-90º, GCD), Lomax and Michelini (2009) have shown that the frequency is high, the duration of rupture, T0, is greater than about 50 or T0 is greater (65) (Madlazim 2011 ; Madlazim, 2013 Madlazim et al., 2015), strengthens the accuracy of tsunami early warning. Lomax and Michelini (2009) exploit this result through direct "duration-exceedance" (DE) procedures applied to seismograms on GCD

10-30º to determine quickly whether T0 for earthquakes tends to exceed 50-55 s and thus become a potentially tsunami earthquake. Madlazim et al., (2015) implemented the Lomax and Michelini (2009) tele-seismic method to measure T0 and T50Ex (DE) with a 65-second threshold for T0, 1 for T50Ex and 10 seconds for the dominant period (Td).

2. METHODS

To achieve the objectives of this study the ADDIE model (Aldoobie, 2015) is used, which consists of 5 stages; Phase of Analysis, Design, Develop, Implementation and Evaluation. The first stage is the Analysis stage. After this stage is completed, then the results are evaluated. The second stage is the Design stage. After this stage is completed, then the results are evaluated. The third stage is the Develop stage. After this stage is completed, then the results are evaluated. The fourth stage is the Implementation stage. After this stage is completed, then the results are evaluated. The fifth stage is the Evaluation stage. This evaluation phase is carried out for all stages.

The five stages in this ADDIE model are as follows: **1. Analysis Phase;** the main activity is to analyze the need to develop a Tsunami Early Warning Application about 4 minutes after the Origin Time of the Earthquake and analyze the feasibility and requirements for developing the application. The existence of problems in the system that have been implemented is not relevant to the needs of the target, technology, and the availability of real-time seismogram data. **2. Designing Phase.** The designing phase is the activity of designing a Tsunami Early Warning Application about 4 Minutes after the Origin Time of the Earthquake. The design of this application is still conceptual and will underlie the next development process. **3**. **Development Phase**. The Development phase contains the realization of product's design activities. The conceptual framework of the Tsunami Early Warning Application of around 4 Minutes after the Origin Time of the Earthquake is compiled and realized into a product that is ready to be implemented. For example, in the designing phase, the designed application is still conceptual, so that at the development stage, the application and the device are made to be ready to be implemented. **4. Implementation Phase.** At this stage, the Tsunami Early Warning Application after 4 Minutes of the Origin Time of the Earthquake is implemented in a real and relevant situation (Meteorology Climatology and Geophysics Council) and an initial evaluation is carried out to provide feedback on the next application. The used real-time data to estimate the earthquake and tsunami parameters is taken from data recorded by a network of local seismic stations managed by the Meteorology Climatology and Geophysics Council. The implementation process for determining tsunami parameters has been integrated with the Indonesian Tsunami Early Warning System known as InaTews (Madlazim, Prastowo, and Hardy 2015). **5. Evaluation Stage.** The Evaluation phase this is done at the processing stage and at the end of the activity. Each end of the stage is evaluated and at the end of the previous four stages, an evaluation is also carried out. Revisions are made according to the evaluation results or needs that cannot be fulfilled by the application yet.

3. RESULTS AND DISCUSSION

The results of this development study can be divided into 2, namely the results in the form of a tsunami early warning application 4 minutes after the earthquake's origin time whose output is presented in Figure 1 and Figure 3 and the results of the application's appropriateness. The output of tsunami early warning application 4 minutes after the earthquake's origin time is in Figure 1 below. In the example of the output of the tsunami early warning application new version is an additional display of the earthquake focal mechanisms that are determined in real time. The focal mechanism can be used as one of the additional information for consideration in making decisions about the potential of a tsunami generated by an earthquake.

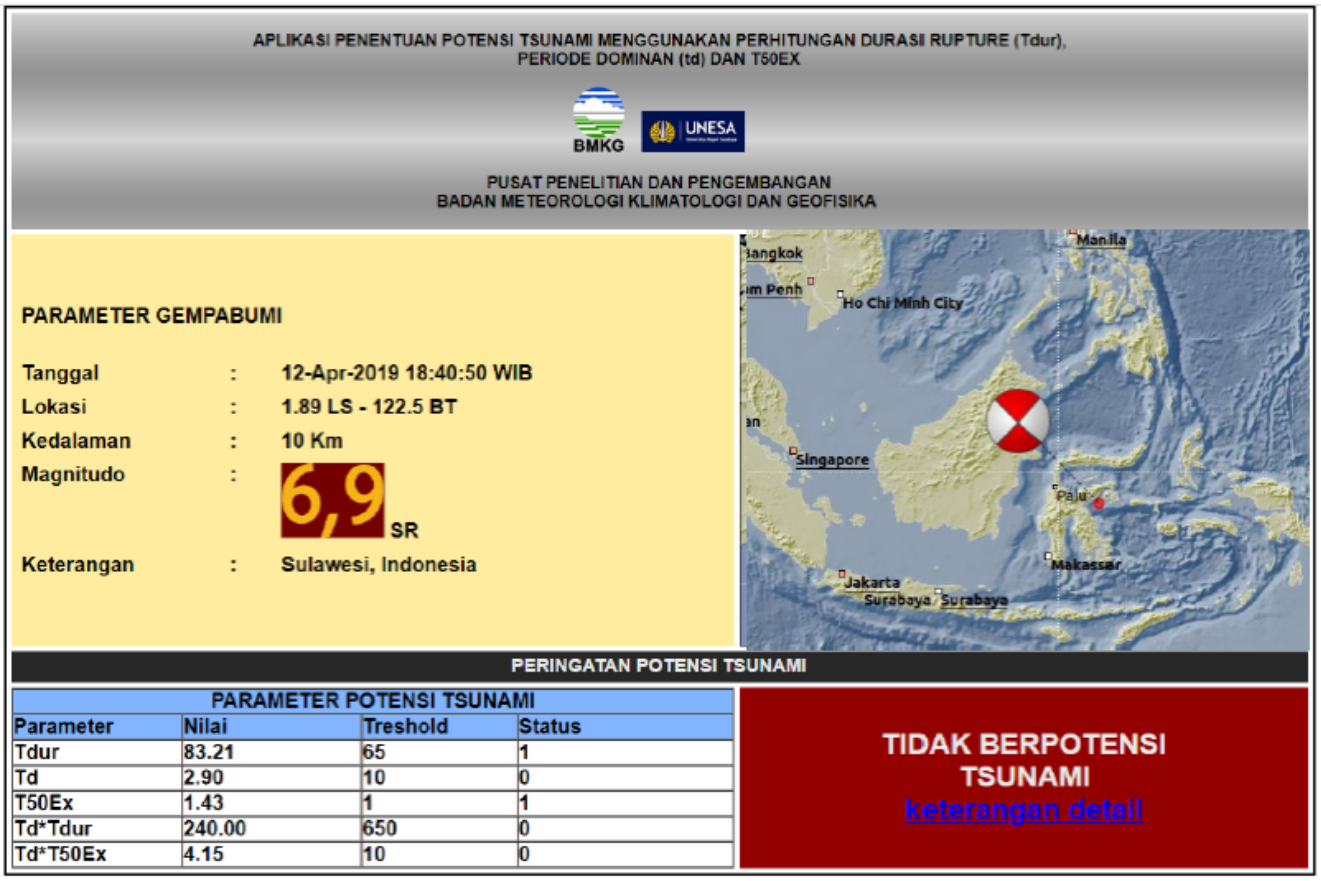

Figure 1. Examples of output from the Tsunami Application 4 minutes after the earthquake equipped with a focal mechanism for August 12th, 2019 earthquake and there is NO TSUNAMI POTENTIAL

The determination of focal mechanism in real time by using the HASH 1.2 method can be accessed free on the web https://earthquake.usgs.gov/research/software/#HASH. To determine the focal mechanism of an earthquake, it takes UP or DOWN data from first motion, phase data, epicentral distance data, take-off beam and azimuth angle from each of Indonesia's local seismic stations managed by Meteorology Climatology and Geophysics Council. Then, by setting the control file, the focal mechanism can be determined. For example, the output is the earthquake focal mechanism that occurred on the Sulawesi Sea on 12th of April 2019 with magnitude 6.9 as shown in Figure 1. From the 5 tsunami parameters, only two

tsunami parameters have slightly exceeded the threshold of Tdur and T50Ex. Whereas the other 3 tsunami parameters (Td, Td * T50Ex and Td * Tdur) do not exceed the threshold, so the tsunami early warning application 4 minutes after the origin time decides there is NO TSUNAMI POTENTIAL. Clearly, the earthquake focal mechanism was strike-slip. Focal earthquake strike-slip mechanism can also cause tsunami (Tanioka and Satake 1996). The output of the focal mechanism from the April 12th, 2019 earthquake has been confirmed by the focal mechanism for the same earthquake in the GLOBAL CMT catalogue (https://www.globalcmt.org/CMTsearch.html) and the results are almost no significant difference. Therefore, the addition of the focal mechanism display in the application of early warning 4 minutes after the origin time further adds to the accuracy of the tsunami application. This application provides information certainty faster (about 4 minutes after origin time), whether an earthquake causes a tsunami or not, so that if needed, a mitigation or evacuation process can be prepared and carried out immediately.

The test of the tsunami early warning application in Palu on 28th of September 2018 was carried out in real-time, also by using local seismic stations as shown in figure 2 to determine tsunami parameters for the September 28th 2018 earthquake.

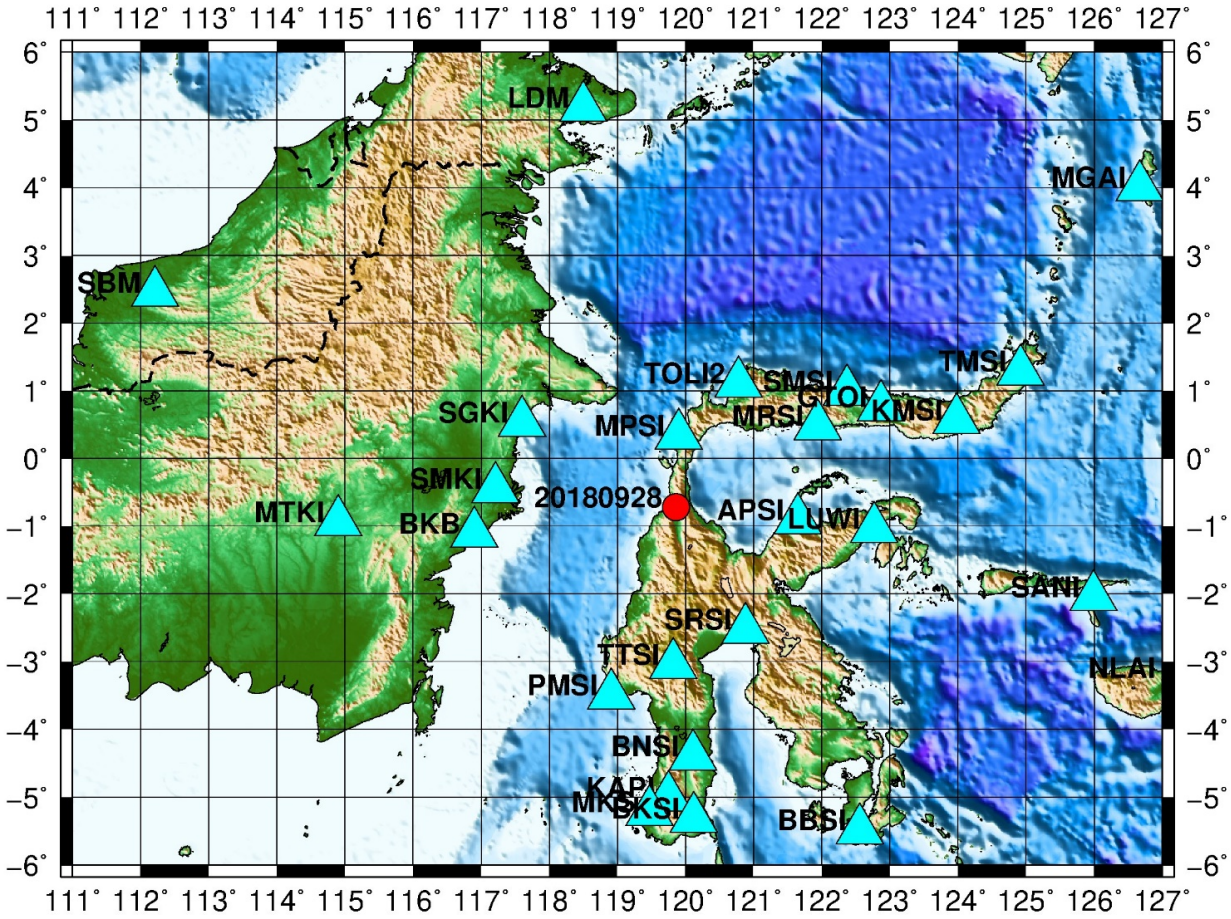

Figure 2. Distribution of the local seismic station (cyan triangle) used by the tsunami application to determine the parameters of the tsunami earthquake in Palu, Indonesia on September 28th, 2018 with the earthquake epicenter (red points).

The use of local stations as shown in Figure 2 allows the results of measuring tsunami parameters (Tdur, Td, and T50Ex) to become available and be announced before 4 minutes, after the origin time of the earthquake. To maintain the accuracy of the measurement results of the tsunami parameters, M-filters were installed (Madlazim et al. 2018). The results of the pilot prototype of the tsunami early warning application 4 minutes after the earthquake in real time for the last 300 earthquakes that occurred in Indonesia (Fig. 4), did not occur in any false warnings.

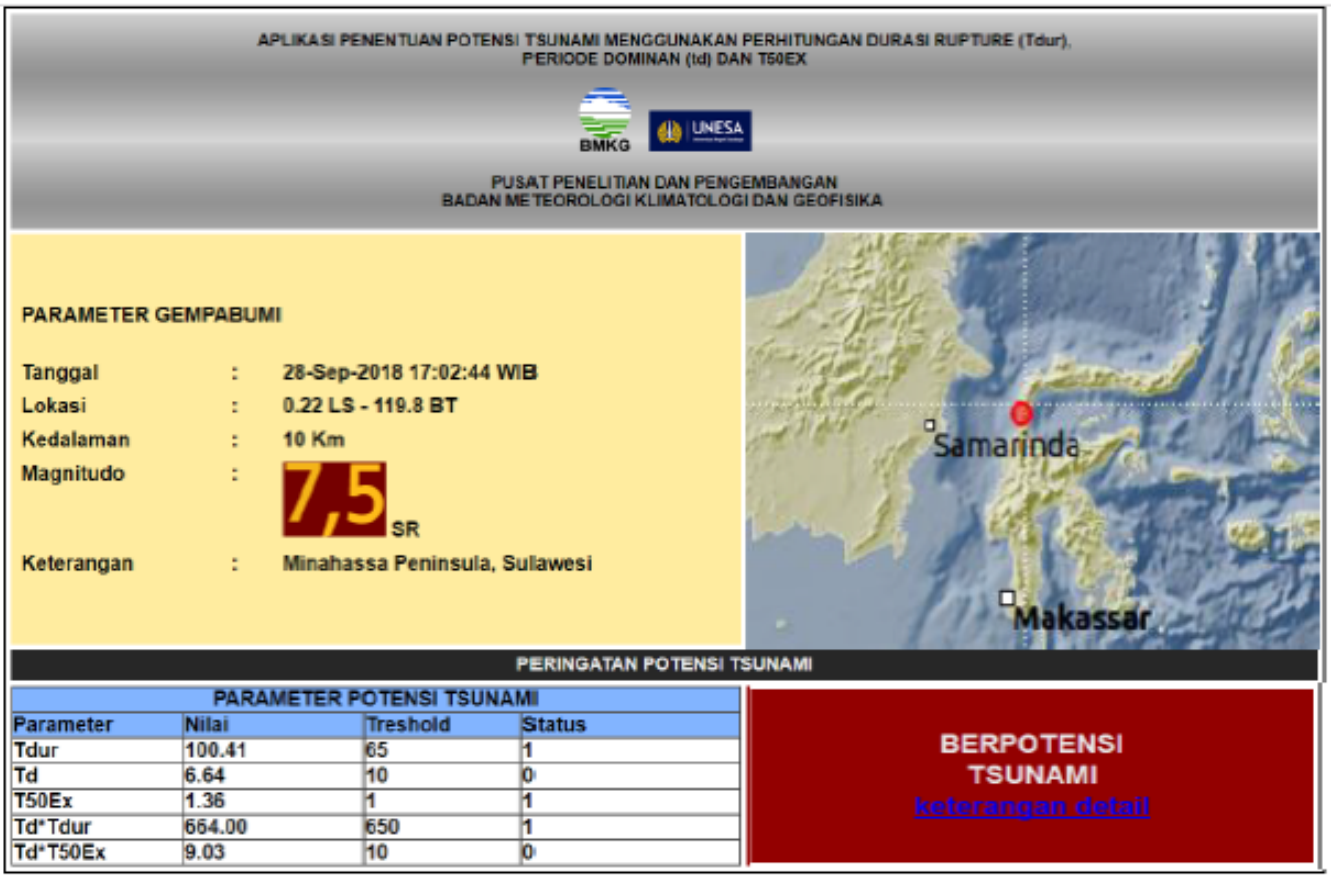

Figure 3. Output of the tsunami early warning application 4 minutes after the earthquake for an earthquake in Palu Indonesia on September 28th, 2018 and there is a TSUNAMI POTENTIAL

The last 300 earthquakes are used for testing the tsunami early warning applications 4 minutes after the earthquake (the yellow epicenter) that occurred in Indonesia starting on June 12th, 2018 until July 20th, 2019 with the magnitude of the earthquakes ranging from 4 to 7.5. The distribution of the earthquake epicenter is presented in Figure 4 as follows.

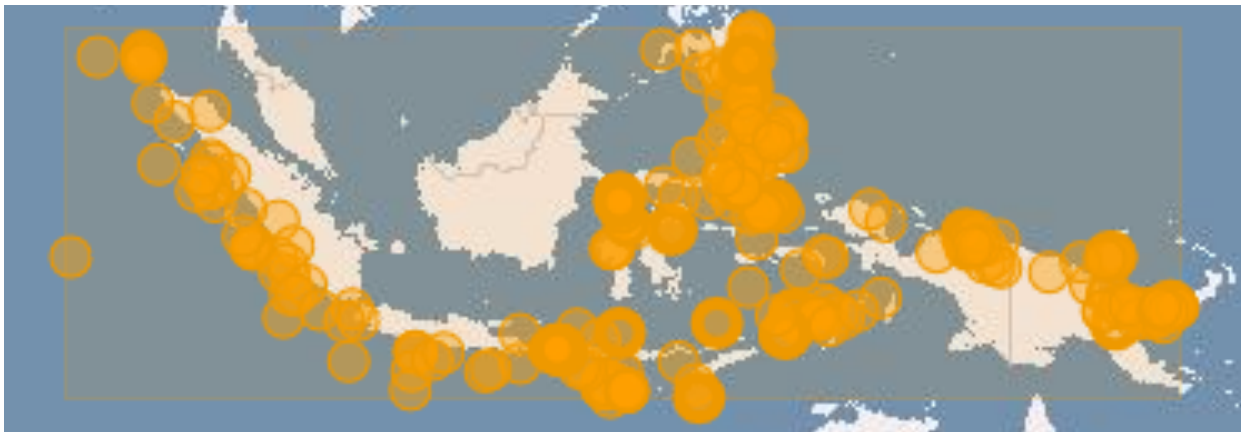

Figure 4. Distribution of earthquake epicenters that occurred in Indonesia from 12th of June 2018 to 20th of July 2019 which are used for testing tsunami applications 4 minutes after the earthquake.

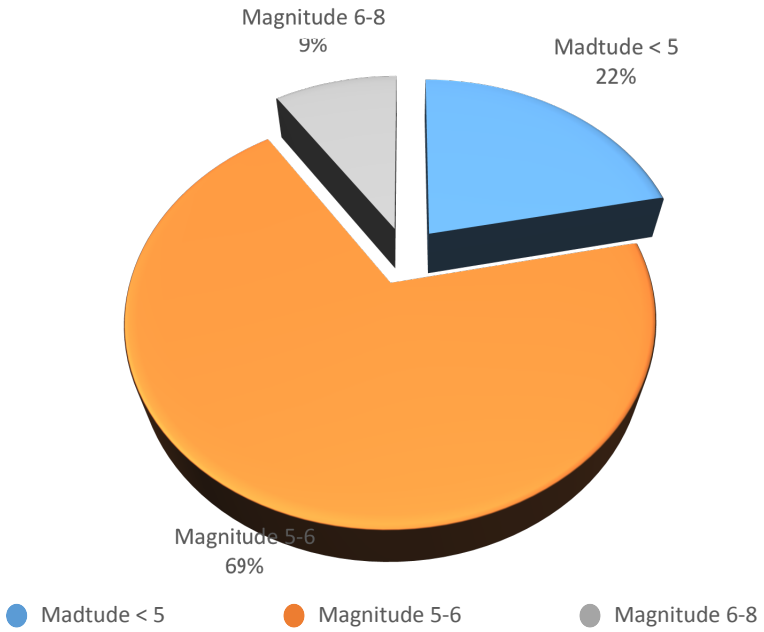

Figure 5. The magnitude of earthquakes that occurred in Indonesia from 12th of June 2018 to 20th of July 2019 which are used for testing the tsunami application 4 minutes after the earthquake.

Figure 5 shows the distribution of magnitude for the earthquakes that are used in the trial. Earthquakes with magnitudes less than 5 are 65 (9%) of the total used earthquakes and for earthquakes with magnitudes of 5 to 6 are 207 (69%). The total earthquakes with magnitude less than 6 are 272 (78%). For the of the tsunami applications previous versions, earthquakes with magnitude less than 6 often occurred false warnings (Madlazim, Prastowo, and Hardy 2015), but for early tsunami mitigation applications 4 minutes after the earthquake, there is no false warning. Whereas for earthquakes with magnitudes 6 to 8 there are 28 (22%). Based on the results of the tsunami early warning application output there is only one earthquake that generate a tsunami, the earthquake that occurred in Palu on 28th September 2018 (Fig. 3).

4. CONCLUSIONS

Tsunami early warning application 4 minutes after the earthquake has been developed and tested in real time at the research and development centre of Meteorology Climatology and Geophysics Council, Jakarta, INDONESIA by using 300 earthquakes that occurred in Indonesia since June 12th, 2018 to July 20th 2019. The results of the tests indicate that tsunami early warning applications 4 minutes after the earthquake meets the eligibility requirements.

Acknowledgment

This work was supported by a research grant, Contract No. 21861/UN38.9/LK.0.4.00/2019" by Ministry of Research, Technology and Higher Education of the Republic of Indonesia. Thank you to the Meteorology Climatology and Geophysics Council for being willing to cooperate in the trial of the tsunami early warning application 4 minutes after this earthquake.

REFERENCES

Aldoobie, N. (2015). ADDIE Model Analysis phase. *American International Journal of Contemporary Research*, *5*(6), 68–72.

Duputel, Z., Rivera, L., Kanamori, H., Hayes, G.P., Hirshorn, B., and Weinstein, S. (2011), Real-time W phase inversion during the 2011 off the Pacific coast of Tohoku Earthquake, *Earth Planets Space*, 63(7), 535-539.

Ekström, G., Dziewonski, A.M., Maternovskaya, N.N., and Nettles, M. (2005), Global seismicity of 2003: Centroid-moment-tensor solutions for 1087 earthquakes, *Phys. Earth Planet. Inter.*, *148*, 327–351.

Lomax, A., Michelini, A. and Piatanesi, A. (2007), An energy-duration procedure for rapid determination of earthquake magnitude and tsunamigenic potential, *Geophys. J. Int.*, *170*, 1195-1209, doi:10.1111/j.1365-246X.2007.03469.x

Lomax, A. and Michelini, A. (2009A), *M*wpd: A duration-amplitude procedure for rapid determination of earthquake magnitude and tsunamigenic potential from *P* waveforms, *Geophys. J. Int.*, *176*, 200–214, doi:10.1111/j.1365-246X.2008.03974.x

Lomax, A. and Michelini, A. (2009B), Tsunami early warning using earthquake rupture duration, *Geophys. Res. Lett.*, *36*, L09306, doi:10.1029/2009GL037223

Lomax, A. and Michelini, A. (2011A), Tsunami early warning using earthquake rupture duration and *P*-wave dominant period: the importance of length and depth of faulting, *Geophys. J. Int.*, *185*, 283–291, doi: 10.1111/j.1365-246X.2010.04916.x

Lomax, A. and Michelini, A. (2011B), Erratum, *Geophys. J. Int.*, *186*, 1454, doi:

10.1111/j.1365-246X.2011.05128.x

Lomax, A. and Michelini, A. (2012), Tsunami Early Warning Within Five Minutes. Pure and Applied Geophysics, Volume 170, Issue 9–10, pp 1385–1395.

Madlazim. 2011. “Toward Indonesian Tsunami Early Warning System by Using Rapid Rupture Duration Calculation,.” *SCIENCE OF TSUNAMI HAZARDS*.

Madlazim, M., Tjipto Prastowo, and Thomas Hardy. 2015. “Validation of Joko Tingkir Software Using Tsunami Importance.” *Science of Tsunami Hazards*.

Madlazim, T. Prastowo, S. Rohadi, and T. Hardy. 2018. “Filter-M Application for Automatic Computation of P Wave Dominant Periods for Tsunami Early Warning.” *Science of Tsunami Hazards*.

Madlazim. 2011. “Toward Indonesian Tsunami Early Warning System by Using Rapid Rupture Duration Calculation,.” *SCIENCE OF TSUNAMI HAZARDS*.

Madlazim, M., Tjipto Prastowo, and Thomas Hardy. 2015. “Validation of Joko Tingkir Software Using Tsunami Importance.” *Science of Tsunami Hazards*.

Madlazim, T. Prastowo, S. Rohadi, and T. Hardy. 2018. “Filter-M Application for Automatic Computation of P Wave Dominant Periods for Tsunami Early Warning.” *Science of Tsunami Hazards*.

Tanioka, Yuichiro, and Kenji Satake. 1996. “Tsunami Generation by Horizontal Displacement of Ocean Bottom.” *Geophysical Research Letters*.

Moore, G. F., Bangs, N. L., Taira, A., Kuramoto, S., Pangborn, E., Tobin, H. J. (2007), Three- Dimensional Splay Fault Geometry and Implications for Tsunami Generation. *Science* 318, 1128, DOI: 10.1126/ science.1147195

Nakamura, Y. (1988), On the urgent earthquake detection and alarm system (UrEDAS), *Proc. of the 9th World Conference on Earthquake Engineering*, Tokyo-Kyoto, Japan.

Newman, A.V., and Okal, E.A. (1998), Tele-seismic Estimates of Radiated Seismic Energy: The E/M_0 Discriminant for Tsunami Earthquakes, *J. Geophys. Res.*, **103** (11), 26,885- 98.

Newman, A.V., Hayes, G., Wei, Y., and Convers, J. (2011), The 25 October 2010 Mentawai tsunami earthquake, from real-time discriminants, finite-fault rupture, and tsunami excitation, *Geophys. Res. Lett.*, *38*, L05302, doi:10.1029/2010GL046498.

Ozaki, T. (2011), Outline of the 2011 off the Pacific coast of Tohoku Earthquake (Mw 9.0) - Tsunami warnings/advisories and observations, *Earth Planets Space*, *63*, 827–830, doi:10.5047/eps. 2011.06.029

Polet, J., and Kanamori, H. (2009), Tsunami Earthquakes, in *Encyclopedia of Complexity and Systems Science*, edited by A. Meyers, Springer, New York, 10370pp., doi:10.1007/978- 0-387-30440-3_567

PTWC (2009), Tsunami Bulletin Number 001, issued at 1830Z 19 MAR 2009, Pacific Tsunami Warning Center/NOAA/NWS.

Satake, K. (2002), Tsunamis, in *International Handbook of Earthquake and Engineering Seismology*, pp. 437–451, eds W.H.K. Lee, H. Kanamori, P.C. Jennings & C. Kisslinger, Academic Press, Amsterdam.

Tanioka, Yuichiro, and Kenji Satake. 1996. “Tsunami Generation by Horizontal Displacement of Ocean Bottom.” *Geophysical Research Letters*.

Tsushima, H., Hirata, K., Hayashi, Y., Tanioka, Y., Kimura, K., Sakai, S., Shinohara, M., Kanazawa, T., Hino, R., and Maeda, K. (2011), Near-field tsunami forecasting using offshore tsunami data from the 2011 off the Pacific coast of Tohoku Earthquake, *Earth Planets Space*, *63*, 821–826.

ISSN 8755-6839

SCIENCE OF **TSUNAMI HAZARDS**

Journal of Tsunami Society International

Volume 38 Number 3 2019

EARTHQUAKE OF 21 FEBRUARY 2011 IN NEW ZEALAND
Generation of Glacial Tsunami

George Pararas-Carayannis
Tsunami Society International

ABSTRACT

An earthquake with Richter magnitude 6.3 struck in the vicinity of Christchurch in New Zealand. It was the second largest seismic event to strike the area within a short time interval. Although of relatively small magnitude, the quake was extremely destructive as it struck much closer to the city than the previous earthquake of 4 September 2010. More than 180 people lost their lives. The earthquake occurred onshore, so there was no tsunami generated. Loss of power at the tide gauge of Lyttelton Port of Christchurch failed to record any wave activity. The GeoNet site at Sumner Head, which is located on the open coast, registered some longer period waves, but these were the result of weather related generation and not of seismic origin. According to eyewitnesses, the earthquake's motions were mild in Aoraki Mt. Cook National Park on the western side of New Zealand's South Island, but the shaking triggered an icefall off the end of the Tasman Glacier's lake and generated significant tsunami waves with an initial wall of water that was 50 or 60 meters high, but up to 3.5 meters high along its shores. The present study assesses the tectonic stresses and seismicity of the Marlborough fault system along the northern part of South Island, and briefly evaluates the potential of future tsunami generation from earthquakes that may be generated near New Zealand's Hikurangi Trough, that may also impact the coasts of South Island as well as the coastlines near the City of Wellington on North Island.

Keywords: *New Zealand earthquakes; glacial tsunami; Christchurch; Wellington; Canterbury area; Hikurangi Trough; Marlborough fault system; Alpine Fault; Puysegur Trench; Tasman Glacier lake.*

1. INTRODUCTION

A shallow focus earthquake occurred on 21 Feb 2011, (UTC 12:51, 22 Feb 2011 NZDT local time and date) at the Canterbury Plains near the city of Christchurch, the largest city of South Island of New Zealand. The seismic region where this earthquake occurred includes the southwest part of South Island (known as Fiordland) and extends offshore to the southwest covering the adjacent Puysegur Trench, which marks the tectonic boundary where the Pacific and Australian plates collide (Pararas-Carayannis, G. 2016 a, b).

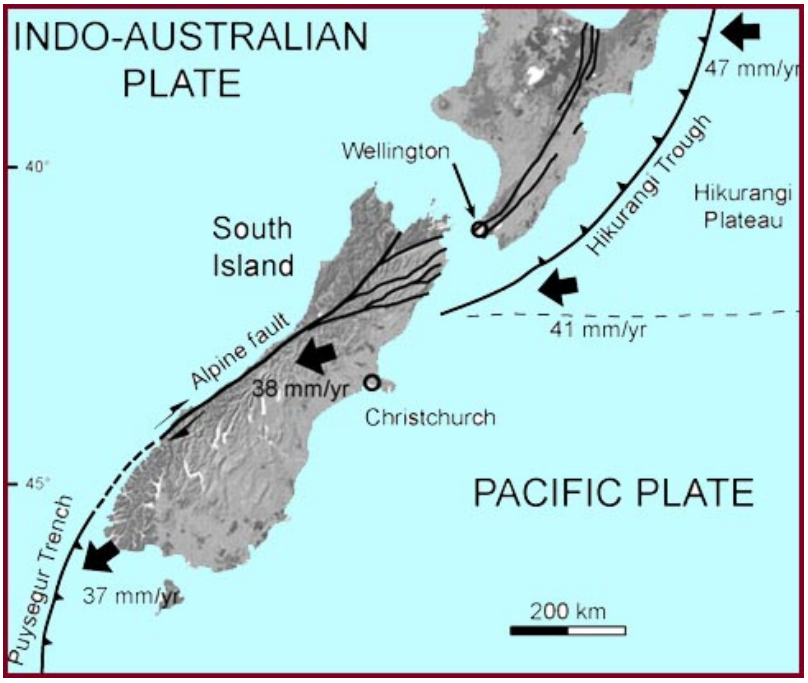

Although the earthquake's magnitude was only 6.3, it was extremely destructive to the city of Christchurch. The earthquake had a shallow rupture and its focal mechanism indicated that it was mainly a strike-slip event. Five months earlier, in September 2010, a stronger earthquake had struck 40 kms west of Christchurch, near the town of Darfield, but did not cause significant damage.

Fig 1. Map of the Indo-Australian plate and of major faults, trenches and troughs, as well as the directions and rates of tectonic movements

No open coast tsunami was generated, but the strong ground motions triggered a significant icefall (a glacial tsunami) off the end of the Tasman Glacier's lake which generated significant waves along its shores. A subsequent study examines the potential of tsunami generation from earthquakes occurring near the Macquarie Fault and Alpine fault zones, the Puysenguir Trench, the Marlborough fault system, the North Island fault system, the Hikurangi Trough of the lower Kermadec Trench (Fig 1, 2). Additionally, prehistoric tsunamis from cascading nuée ardentes and pyroclastic volcanic flows into the Bay of Plenty on the North Island and elsewhere in New Zealand will be examined.

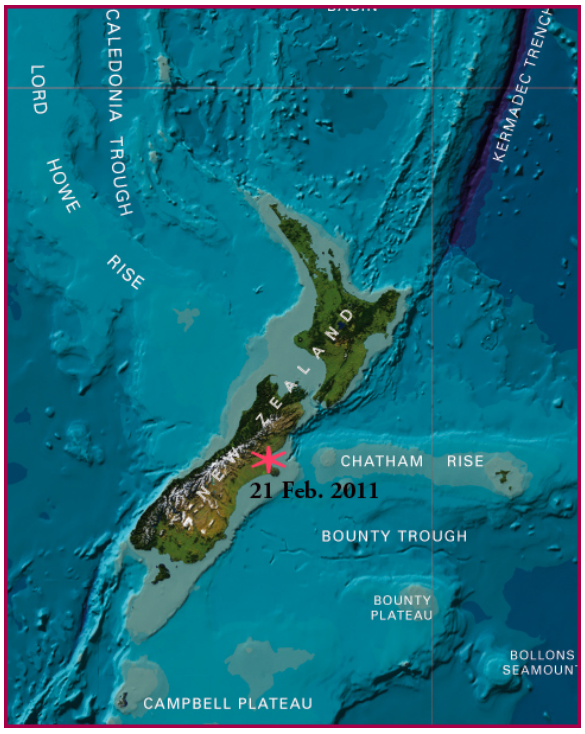

Fig 2. Epicenter of the 21 February 2011 Earthquake

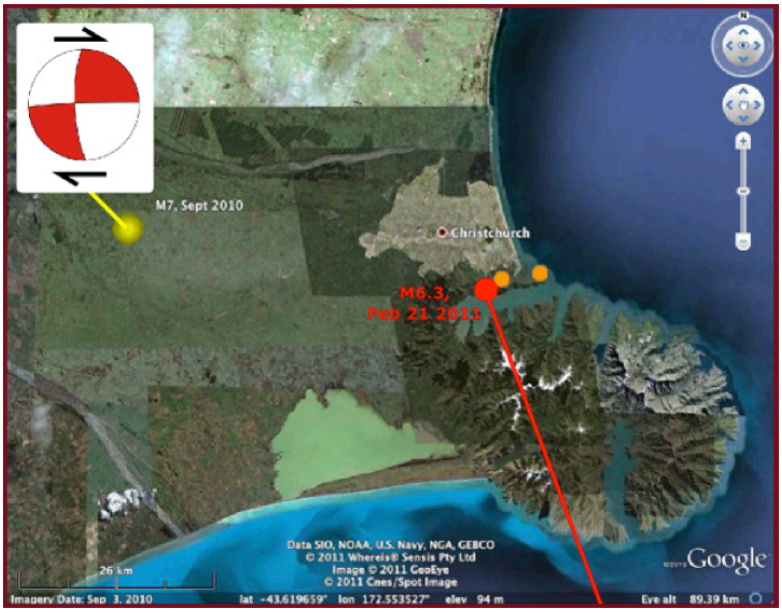

2. THE EARTHQUAKE OF 21 FEBRUARY 2011

Date, Time, Epicenter, Magnitude and Rupture - The earthquake had moment magnitude M_w 6.2 (M_L 6.3). It occurred at 23:51 on 21 February 2011 UTC (12:51, 22 Feb 2011 NZDT local time and date). Its epicenter (Fig. 2 & 3) was at the Canterbury Plains about 6.7 km from the center of Christchurch, New Zealand - the largest city of South Island, which is over 100 Kms from the Alpine fault.

Fig 3. Epicenters of the M7 4 September 2010 and of the M6.3 21 February 2011 earthquakes near Christchurch (NOAA graphic)

Its shallow rupture and its focal mechanism indicated that it was mainly a shallow, strike-slip event. The earthquake was felt across the South Island and parts of the lower and central North Island.

The seismic region where this earthquake occurred includes the Southwest part of South Island (known as Fiordland) and extends offshore to the Southwest covering the adjacent Puysegur Trench, which marks the tectonic boundary where the Pacific and Australian plates collide (Fig. 1).

Aftershocks - There were many strong aftershocks following the main earthquake. Two strong aftershocks occurred on Monday, 14 June 2011, nearly four months after the 21 February 2011 main quake. According to USGS data, the first was a shallow event with depth of 11 km and had magnitude of 5.2 and epicenter about 9 km (5 miles) east-southeast of the main event. A second quake occurred 90 minutes later. It was also shallow (focal depth 9 km) and had a Richter magnitude 6.0. Its epicenter was — about 13 kilometers (8 miles) north-northeast of Christchurch (Fig. 3).

Loss of Life and Damages - There was severe destruction to the city of Christchurch. It was particularly damaging because it was a shallow quake near a densely populated area. The strong ground motions caused the collapse of the Canterbury Television building killing 115 people. Significant liquefaction affected the eastern suburbs, producing around 400,000 tonnes of silt.

Remaining Seismic Stress in the Christchurch Region After the Earthquake - The earthquake of 22 February 2011 near Christchurch, did not appear to have released all its energy (Pararas-Carayannis, G. 2016 a, b). Also, it raised the question on whether it occurred on a new fault or along a previously Un-recognized fault — an offshoot from the Alpine fault — that did not rupture in recent geologic times and thus there was no historic data. Although the earthquake of 22 February 2011 had a moderate magnitude of 6.3, and tremors lasted for only ten-seconds, what made it worse was the fact that it occurred close to the city of Christchurch where buildings had been weakened — and not subsequently upgraded — by an earlier 7.1 event of 4 September 2010 in the region (Fig 3).

Also, the 22 February 2011 quake and a subsequent event on 24 July 2016 - both near Christchurch - raised the question on whether all accumulated stress in the region was released, or whether additional quakes could be expected. The progression of subsequent earthquakes in the region, indicated that energy was transferred to adjacent faults — as indeed it happened in 2016 (Pararas-Carayannis, 2016 a, b). More earthquakes with local tsunamigenic potential were expected near South Island with additional adverse impact in the Christchurch and in the Wellington area of North Island. Several of the active faults that may be present in this region have not been adequately identified.

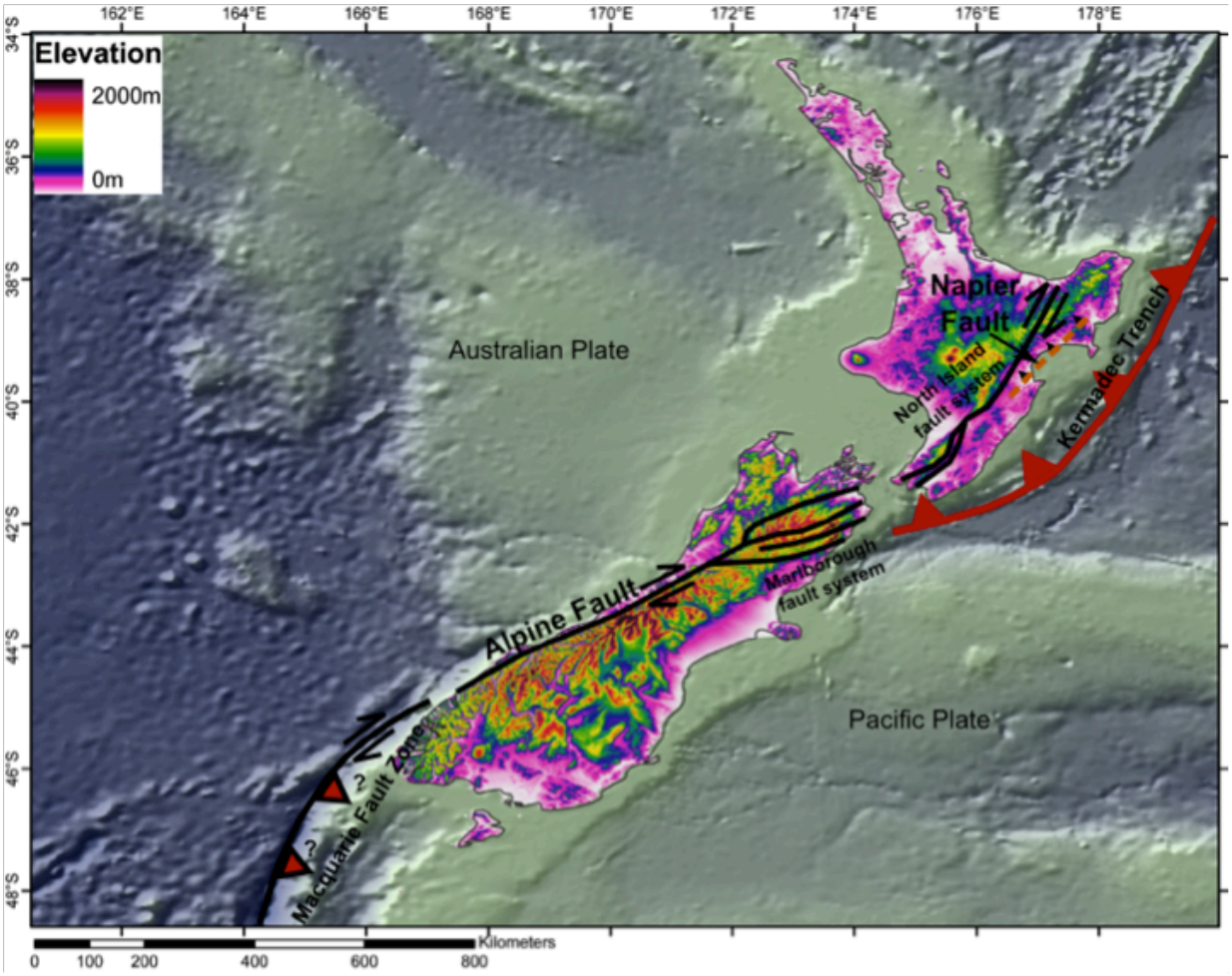

Fig 4. The Macquarie Fault and Alpine fault zones, the Puysenguir Trench, the Marlborough fault system, the North Island fault system, the Hikurangi Trough of the lower Kermadec Trench.

Subsequently, on 1 September 2016, a magnitude 7.2 earthquake occurred off the East coast of North Island. However this quake had a deep focal depth of 99 miles, thus did not pose a threat of tsunami generation or of damage from surface seismic waves. Based on assessment of tectonic stresses, the present study postulated that subsequent major earthquakes in the region could occur that could also impact the capital city of Wellington. The following section provides a brief review of some of the major and large

earthquakes that have occurred in New Zealand in relatively recent times — some generating destructive tsunamis. As previously stated a subsequent study in preparation examines the potential of tsunami generation from earthquakes occurring near the Macquarie Fault and Alpine fault zones, the Puysenguir Trench, the Marlborough fault system, the North Island fault system, the Hikurangi Trough of the lower Kermadec Trench (Fig. 1, 4) — as well as prehistoric tsunamis from volcanic sources.

3. PREVIOUS AND SUBSEQUENT LARGE EARTHQUAKES IN NEW ZEALAND - A Brief Review.

Given the nature of the geology, earthquakes in New Zealand along the tectonic boundary where the Pacific and Australian plates collide are common, although those of magnitude 7.0 or more are relatively infrequent. A list of large earthquakes which have occurred in New Zealand is provided by Wikipedia (https://en.wikipedia.org/wiki/List_of_earthquakes_in_New_Zealand). Only earthquakes with a magnitude of 6.0 or greater are listed, except for a few that had a moderate or severe impact. Aftershocks are not included, unless they were of great significance or contributed to a death toll, as that of the 2011 Christchurch earthquake discussed in this paper.

3a. Large Historical Earthquakes and Tsunamis - The largest recorded earthquake in New Zealand took place in 1855 at Wairapa and had a magnitude of 8.2. Earthquakes of 7.8 magnitude have caused significant damage and some loss of life in 1848, 1929 and 1931. The major earthquakes that affected the broader region of Canterbury Province occurred in 1888 and in 1929. In more recent times, the same Canterbury area has been impacted by earthquakes of M5.9 and M6.7 in 1994 (USGS; GeoNet; Pararas-Carayannis, 2016 a, b). In July 2009 an earthquake of M7.8 occurred in the South Island's relatively uninhabited west coast region. The next section reviews briefly only the more recent larger earthquake events - some having generated tsunamis.

1931- FEBRUARY - 3 - The "Napier earthquake" of 3 February 1931 was the worse natural disaster in New Zealand. It caused many deaths, injured thousands of people and caused severe destruction, not only in the Hawke's Bay Region of North Island but on South Island as well. According to a 1931 *New Zealand Listener* article, this quake resulted in 258 deaths, which included two missing people - presumed dead. The epicenter of the 1931 quake was about 15 km north of the town of Napier. Its magnitude was estimated at 7.8 M_s (moment magnitude 7.9 M_w), and the ground motions lasted for two and a half minutes. The quake was a strike-slip event (Mouslopoulou et.al, 2007; Pararas-Carayannis, 2016 a, b). There were 525 aftershocks recorded in the following two weeks, with 597 being recorded by the end of February 1931. The main shock and many of the aftershocks were felt throughout New Zealand, and according to GeoNet as far south as Timaru, on the East coast of South Island.

1979 - OCTOBER 12 - A thrust earthquake with magnitude 7.3 occurred offshore near the Puysegur Trench to the southwest of South Island.

2003 - AUGUST 21- This was a shallow earthquake which occurred in Fiordland - a remote seismically active region in the southwest of the South Island. It was a thrust event had a moment magnitude M_w7.2 . the largest to occur in New Zealand in 35 years (Reyners, et.al., 2003; McGinty, 2003).

2004 - NOVEMBER 22 - This earthquake occurred off the West coast of South Island on 22 November 2004 at 20:26:23 UTC and had a magnitude 7.1 and a relatively shallow depth (NEIC). No tsunami was generated.

2010 - SEPTEMBER 4 - A severe earthquake - subsequently named as the Canterbury earthquake of 2010 - struck near the city of Christchurch, at the South Island. No fatalities were reported for this quake but there was considerable damage to buildings in and around Christchurch. It appears that the origin of this quake was along one of the two major faults, the Hope Fault and the Alpine Faults, which run along the South Island and are the main expression of the boundary between the Pacific and Indian (or Indo-Australian) tectonic plates (Pararas-Carayannis, 2016 a, b). The Richer magnitude of this event was estimated as M7.0 (USGS)(also reported locally as 7.1) - making it one of the strongest in 2010. The USGS reported that it was lateral (strike-slip) movement that caused it (Fig 3). The epicenter was between 40-50 km west Christchurch (sources vary) and was followed by numerous aftershocks for a period of days and weeks. At least thirty of these aftershocks had magnitudes of at least M4.0. There was a strong tremor of M5.1 on 8 September 2010 and another one of M5.0 on 19 October 2010. However, the October event was too strong and too far in space and time to be considered as an aftershock.

2016 - NOVEMBER - 14 - This event known as the 2016 Kaikoura earthquake, had a moment magnitude 7.8 (M_w) (US Geological Survey, 2016; GeoNet, 2016). It occurred on 14 November 2016 NZDT (11:02 on 13 November UTC) near the towns of Culverden and Kaikoura, and about 95 km from Christchurch. Its focal depth was about 15 kms and it was accompanied by several sequences of ruptures on numerous faults on land and at sea (GeoNet, 2017). The ground motions lasted for about two minutes. Tsunami waves up to 7 meters were documented at Goose Bay. Some other tide gauges that recorded the tsunami waves were in Wellington Harbor, Castlepoint, Christchurch, and the Chatham Islands (Daly, M., 2017) https://en.wikipedia.org/wiki/2016_Kaikoura_earthquake

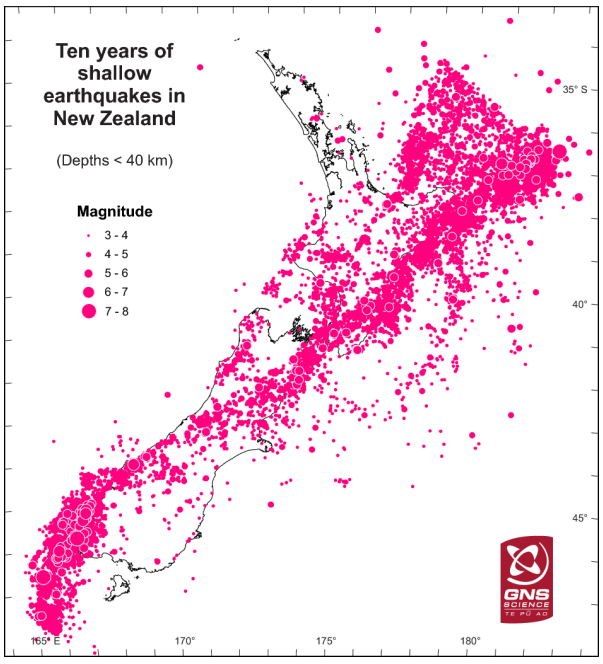

4. SEISMICITY OF NEW ZEALAND - A Brief Review

Active tectonic processes in New Zealand result in thousands of earthquakes every year (Fig 5). However, most of the quakes are too small to be felt and cause no damage.

Fig 5. Distribution of shallow focus earthquakes in New Zealand over a ten year period (source GNS Science).

New Zealand's high frequency of usually small quakes results from its proximity to the broad boundaries where

the tectonic plates of the Pacific and Australian plates collide. North Island is part of the Australian continental plate which is under-thrust by the higher density Pacific Oceanic plate along a zone of subduction. Something similar is occurring south-west of the South Island of New Zealand where sliver of continental crust lies on the Pacific plate, and it is the Australian plate that is being destroyed through subduction (Pararas-Carayannis, 2016 a, b).

In between, the continental crust on the Pacific and Australian plates slide past one another on South Island, creating a conservative plate margin where crust is neither created nor destroyed. This area is still prone to earthquakes, most notably along the Alpine fault to the west of South Island. Further away from these fault zones the ground is generally more quiescent. The historical record indicates that in the last 200 years both North and South Islands of New Zealand have experienced several earthquakes with magnitudes greater than 5, but few of greater magnitudes.

5. GENERATION OF GLACIAL TSUNAMI

The earthquake occurred onshore, so there was no open coast tsunami generated. The Loss of power at the tide gauge of Lyttelton Port of Christchurch failed to record any wave activity. The GeoNet site at Sumner Head, which is located on the open coast, registered some longer period waves but these were the result of weather related generation and not of seismic origin.

The earthquake's ground motions were mild at the Aoraki Mt. Cook National Park on the western side of New Zealand's South Island. However, according to eye-witnesses, the shaking triggered a break of an iceberg off the end of the Tasman Glacier Lake and generated a tsunami (Fig 6).

Fig 6. Photo of iceberg in Tasman Lake at Aoraki Mt. Cook National Park (photo from Glacier Explorers)

The glacier shown in Fig. 6 is similar to the iceberg that calved and collapsed into the Tasman Lake in the Aoraki Mt. Cook National Park right after the earthquake. According to eyewitnesses reports the initial wall of water was 50 to 60 meters in height and boats in the lake experienced big waves for about 30 minutes and that these waves were up to 3.5 meters in height. Subsequent estimates that were provided, mentioned that about 30 million tonnes of ice calved across 1200 meters of the glacier's face. According to the same estimates the glacier's top was 30 meters above the surface of the lake and more than 250 meters below the surface to the bottom of the lake, and its thickness was estimated to be about 75 meters. According to a Mr. Callesen of Glacier Explorers, this event was either the third biggest, or second-equal biggest event in the known history of Tasman Lake.

6. CONCLUSIONSMarlborough

As indicated by the present review of the 21 February 2011 earthquake and of the previous and subsequent events,New Zealand is a region of considerable tectonic complexity. As stated, the country lies on the boundary between two large crustal plates, the Pacific Plate (moving approximately north-east) and the Indian Plate (moving roughly north). New Zealand is located at a transform boundary, where these two plates move laterally past one another, thus resulting in numerous earthquakes. The transform zone runs through both North and South Islands, although towards the North Marlborough the nature of the boundary changes and becomes a subduction zone, characterized also by volcanic activity. Because of New Zealand's proximity to the Alpine fault and the continuous, interactive and large tectonic movements along this great seismic boundary, more earthquakes and local tsunamis can be expected.

The present study helps document the tectonic stresses and seismicity of the Marlborough fault system along the northern part of South Island, and briefly evaluates the potential of future tsunami generation from earthquakes that may be generated near New Zealand's Hikurangi Trough, that may also impact the coasts of South Island as well as the coastlines near the City of Wellington on North Island.

REFERENCES

Daly, M., 2017. "November tsunami up to 7 metres high". *The Press*. p. A4. Retrieved 28 March 2017.

GeoNet - Geological Hazard Information for New Zealand. "M 7.4 Hawke's Bay Tue, Feb 3 1931".

GeoNet - Geological Hazard Information for New Zealand, 2016. "Magnitude 7.8, Mon, Nov 14 2016, 12:02:56 am (NZDT)". GeoNet. Retrieved 16 November 2016.

GeoNet - Geological Hazard Information for New Zealand, 2017. "A year on, how is the Kaikōura aftershock sequence playing out compared to Darfield?". Retrieved 29 November 2017.

McGinty P. 2003. The 2003, MW 7.2 Fiordland Earthquake, and its near- source aftershock strong motion data. Institute of Geological & Nuclear Sciences, PO Box 30-368, Lower Hutt, New Zealand 2004 NZSEE Conference

Mouslopoulou, V; Nicol, A; Little, T. A; Walsh, J. J., 2007. "Terminations of large strike-slip faults: An alternative model from New Zealand", *Geological Society, London, Special Publications*, **290** (1): 387–415, Bibcode:2007GSLSP.290..387M, doi:10.1144/SP290.15

Pararas-Carayannis, G., 2016a. Major Historic Earthquakes in New Zealand. Keynote Presentation. Seventh International Tsunami Symposium (ISPRA-2016)Tsunami Society International, 12-15 Sept. 2016, European Union - Joint Research Centre, Ispra, Italy.

Pararas-Carayannis, G., 2016b. Assessment of Earthquake and Tsunami Vulnerability of New Zealand based on the evaluation of recent events and geotectonic stresses caused by underthrusting of the Pacific Oceanic plate along a zone of subduction. Plenary Presentation. Seventh International Tsunami Symposium (ISPRA-2016), Tsunami Society International, 12-15 Sept. 2016, European Union - Joint Research Centre, Ispra, Italy.

Reyners, M., McGinty, P., Gledhill, K., O'Neill, T., Matheson, D., Cousins, J., Zhao, J., McVerry, G., Cowan, H., Hancox, G., Cox, S., Turnbull, I., Caldwell, G., and the GeoNet team. 2003. The MW 7.2 Fiordland earthquake of August 21, 2003: background and preliminary results. Bulletin of the New Zealand Society for Earthquake Engineering, Bull. N.Z Nat. Soc. Vol. 36: number 4.

U.S. Geological Survey, 2016, "M7.8 – 53km NNE of Amberley, New Zealand". Retrieved 19 November 2016

Wikipedia, 2017. List of Earthquakes in New Zealand. (https://en.wikipedia.org/wiki/List_of_earthquakes_in_New_Zealand)

ISSN 8755-6839

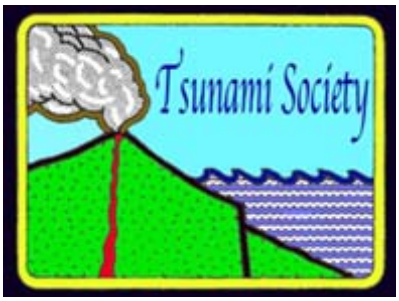

SCIENCE OF **TSUNAMI HAZARDS**

Journal of Tsunami Society International

Volume 38 **Number 3** **2019**

WWW.TSUNAMISOCIETY.ORG

TSUNAMI SOCIETY INTERNATIONAL, 1741 Ala Moana Blvd. #70, Honolulu, HI 96815, USA.

WWW.TSUNAMISOCIETY.ORG